

OECD DOCUMENTS

Physics of Plutonium Recycling

Volume IV

Fast Plutonium-Burner Reactors: Beginning of Life

Benchmark Results Analysis

A report by

*the Working Party on the Physics of Plutonium Recycling
of the NEA Nuclear Science Committee*

The following texts are published in their original form to permit faster distribution at a lower cost.

NUCLEAR ENERGY AGENCY
ORGANISATION FOR ECONOMIC CO-OPERATION AND DEVELOPMENT

ORGANISATION FOR ECONOMIC CO-OPERATION AND DEVELOPMENT

Pursuant to Article 1 of the Convention signed in Paris on 14th December 1960, and which came into force on 30th September 1961, the Organisation for Economic Co-operation and Development (OECD) shall promote policies designed:

- to achieve the highest sustainable economic growth and employment and a rising standard of living in Member countries, while maintaining financial stability, and thus to contribute to the development of the world economy;
- to contribute to sound economic expansion in Member as well as non-member countries in the process of economic development; and
- to contribute to the expansion of world trade on a multilateral, non-discriminatory basis in accordance with international obligations.

The original Member countries of the OECD are Austria, Belgium, Canada, Denmark, France, Germany, Greece, Iceland, Ireland, Italy, Luxembourg, the Netherlands, Norway, Portugal, Spain, Sweden, Switzerland, Turkey, the United Kingdom and the United States. The following countries became Members subsequently through accession at the dates indicated hereafter: Japan (28th April 1964), Finland (28th January 1969), Australia (7th June 1971), New Zealand (29th May 1973) and Mexico (18th May 1994). The Commission of the European Communities takes part in the work of the OECD (Article 13 of the OECD Convention).

NUCLEAR ENERGY AGENCY

The OECD Nuclear Energy Agency (NEA) was established on 1st February 1958 under the name of the OEEC European Nuclear Energy Agency. It received its present designation on 20th April 1972, when Japan became its first non-European full Member. NEA membership today consists of all European Member countries of OECD as well as Australia, Canada, Japan, Republic of Korea, Mexico and the United States. The Commission of the European Communities takes part in the work of the Agency.

The primary objective of NEA is to promote co-operation among the governments of its participating countries in furthering the development of nuclear power as a safe, environmentally acceptable and economic energy source.

This is achieved by:

- *encouraging harmonization of national regulatory policies and practices, with particular reference to the safety of nuclear installations, protection of man against ionising radiation and preservation of the environment, radioactive waste management, and nuclear third party liability and insurance;*
- *assessing the contribution of nuclear power to the overall energy supply by keeping under review the technical and economic aspects of nuclear power growth and forecasting demand and supply for the different phases of the nuclear fuel cycle;*
- *developing exchanges of scientific and technical information particularly through participation in common services;*
- *setting up international research and development programmes and joint undertakings.*

In these and related tasks, NEA works in close collaboration with the International Atomic Energy Agency in Vienna, with which it has concluded a Co-operation Agreement, as well as with other international organisations in the nuclear field.

© OECD 1995

Applications for permission to reproduce or translate all or part
of this publication should be made to:
Head of Publications Service, OECD
2, rue André-Pascal, 75775 PARIS CEDEX 16, France.

FOREWORD

The OECD/NEA Nuclear Science Committee set up a Working Party on Physics of Plutonium Recycling in June 1992 to deal with the status and trends of physics issues related to plutonium recycling with respect to both the back end of the fuel cycle and the optimal utilisation of plutonium. For completeness, issues related to the use of the uranium coming from recycling are also addressed.

The Working Party met three times and the results of the studies carried out have been consolidated in the series of reports "Physics of Plutonium Recycling".

The series covers the following aspects:

- Volume I *Issues and Perspectives;*
- Volume II *Plutonium Recycling in Pressurized-water Reactors;*
- Volume III *Void Reactivity Effect in Pressurized-water Reactors;*
- Volume IV *Fast Plutonium-Burner Reactors: Beginning of Life;*
- Volume V *Plutonium Recycling in Fast Reactors;* and
- Volume VI *Multiple Recycling in Advanced Pressurized-water Reactors.*

The present volume is the fourth in the series and describes the specific benchmark studies concerned with the calculation of physics parameters of both a MOX-fuelled and a metal-fuelled fast plutonium-burner reactor. The analysis concentrates on parameters of initial fuelling ("beginning of life") and their change after a single burnup cycle.

The opinions expressed in this report are those of the authors only and do not represent the position of any Member country or international organisation. This report is published on the responsibility of the Secretary-General of the OECD.

CONTENTS

Summary	7
Contributors and benchmark participants	9
Introduction	11
Beginning of cycle oxide-fuelled fast burner.....	12
Specification.....	12
Results	12
Beginning of cycle metal-fuelled fast burner	14
Specification.....	14
Results	15
Europe.....	15
Japan	16
Russia.....	16
United States.....	16
Comparison of results.....	17
Conclusions.....	19
References.....	20
Tables and Figures	21
Appendix A Specification of a fast plutonium-oxide burner reactor benchmark configuration (600 MWe)	45
Appendix B Specification of metal-fuelled benchmark.....	53
List of symbols and abbreviations	65

SUMMARY

Fast reactor physics benchmarks were developed as part of a programme of the OECD/NEA Working Party on Physics of Plutonium Recycling (WPPR) to evaluate different scenarios for the use of plutonium.

Fast burner fuel cycle scenarios using either PUREX/TRUEX (oxide fuel) or pyrometallurgical (metal fuel) separation technologies were specified. These benchmarks were designed to evaluate the nuclear performance, and the reduction of waste radiotoxicity achievable in a transuranic-burning fast reactor system.

In this report, benchmark results are summarised for the beginning-of-life cases wherein the geometry and composition are specified and a single burnup step of specified energy extraction is specified. Comparisons of participant's predictions are summarised and key conclusions regarding the size and cause of variabilities among participant solutions are highlighted.

CONTRIBUTORS AND BENCHMARK PARTICIPANTS

AUTHORS	<i>G. Palmiotti</i>	ANL	U.S.A.
	<i>R. Hill</i>	ANL	U.S.A.
	<i>D. Wade</i>	ANL	U.S.A.
PROBLEM SPECIFICATION	<i>J.C. Garnier</i>	CEA	France
	<i>T. Ikegami</i>	PNC	Japan
	<i>D. Wade</i>	ANL	U.S.A.
DATA COMPILATION AND ANALYSIS	<i>G. Palmiotti</i>	ANL	U.S.A.
	<i>R. Hill</i>	ANL	U.S.A.
SECRETARIAT	<i>E. Sartori</i>	OECD/NEA	
TEXT PROCESSING AND OUTLAY	<i>E. Johnson</i>	ANL	U.S.A.
	<i>P. Jewkes</i>	OECD/NEA	
BENCHMARK PARTICIPANTS	<i>J. Da Silva</i>	CEA	France
	<i>J.C. Garnier</i>	CEA	France
	<i>G. Rimpault</i>	CEA	France
	<i>F. Varaine</i>	CEA	France
	<i>T. Ikegami</i>	PNC	Japan
	<i>S. Ohki</i>	PNC	Japan
	<i>T. Yamamoto</i>	PNC	Japan
	<i>M. Kawashima</i>	Toshiba	Japan
	<i>M. Yamaoka</i>	Toshiba	Japan
	<i>S. Pelloni</i>	PSI	Switzerland
	<i>A. M. Tsibulia</i>	IPPE	Russia
	<i>P. Smith</i>	AEA	U.K.
	<i>K. Grimm</i>	ANL	U.S.A.
	<i>R. Hill</i>	ANL	U.S.A.
	<i>G. Palmiotti</i>	ANL	U.S.A.

Introduction

Two fast burner benchmark designs (one oxide and one metal) were specified by the Working Party on Physics of Plutonium Recycling (WPPR). Both designs utilise a power rating of 600 MWe and both employ similar strategies to lower the conversion ratio well below unity. The uranium content in the reactor is reduced both by removing blanket assemblies and by increasing the enrichment of the driver fuel up to the limits of the fuel irradiation data base. The neutrons that otherwise would have been captured on uranium are purposely wasted by dramatically increasing the core leakage fraction. Thus, the neutron balances of these fast burner reactors are quite different from conventional fissile-self-sufficient or breeder designs for which the cross-section data sets and calculational methods have been extensively verified in historical fast breeder reactor development programmes.

The sources of plutonium and other transuranics used to create the beginning-of-life (BOL) loading were selected in a way to span the range of potential sources from the LWR economy in the intermediate time interval prior to widespread commercialisation of fast fissile-self-sufficient or breeder reactor designs. In the case of the oxide benchmark, the feedstream from the thermal reactor cycle is strongly skewed toward heavier plutonium isotopes (e.g., Pu-242 is 14% of total mass). This feedstream is characteristic of a scenario in which the plutonium has been twice recycled (three times burnt) in a thermal spectrum LWR. *Also planned is that during the reprocessing step, the Np and Am will be removed and not recycled in the LWRs, but rather saved for introduction into the fast burner cycle.* In the case of the metal-fuelled benchmark, the feedstream from the thermal reactor cycle represents LWR once-through fuel with about three years of cooling prior to reprocessing and injection into the fast reactor closed fuel cycle; a pyrometallurgical technology to reduce LWR spent fuel and produce a fast reactor metallic feedstream containing all transuranics admixed together (Pu + Np + Am + Cm) is assumed. The plutonium vector is skewed more to the lighter isotopes (only 4% Pu-242) than is the case for the feedstream to the oxide benchmark; however, all minor actinides (Np, Am, and Cm) are included in the feedstream. The core compositions deviate from the traditional ones used in prior breeder reactor development programmes and comprise a further reason to question whether current data sets and methods are adequate.

Since the primary goal of the benchmark activity discussed in this report was to assess the variability among participants' solutions which arises for burner cores the neutron balance and composition of which is substantially altered from that of traditional designs, the beginning-of-life benchmarks fully specified the geometry, the beginning of life composition and the time interval and energy extraction of a single burnup step¹. Basic nuclear data, cross-section generation methods, and neutron balance solution methodology will thus be the sole cause of variations in predicted performance. The benchmark participants were asked to provide computational predictions of beginning-of-life eigenvalue and neutron balance, spectral indices and safety coefficients. Also, the composition and eigenvalue changes after the single burn cycle, and the end-of-cycle decay heat and isotopic contributions to toxicity (using specified toxicity factors) were reported by participants.

¹ The PYRØ recycle-metal-fuelled fast burner benchmark specification comprised not only a beginning-of-life case, but also once-through, and multiple recycle cases as well – see Volume 5.

As shown in Table 1, international design teams submitted six solutions for the oxide-fuelled benchmark and five solutions for the metal-fuelled benchmark.

Beginning-of-life oxide-fuelled fast burner

Specification

The detailed oxide-fuelled benchmark specification is provided in Appendix A; only its main features are described here.

The oxide burner benchmark is a 600 MWe (1500 MWth) burner reactor which operates on a 125 EFPD cycle at 80% capacity factor; one fifth of the core is refuelled per cycle. As shown in Figure 1, the core is of a homogeneous layout with two radial enrichment zones and no radial blankets. Axially, the core is about a meter high and has no axial blankets. The conversion ratio is near 0.5. The fuel comprises an annular mixed oxide pin of depleted uranium and multi-recycled LWR plutonium. The beginning-of-life compositions are specified as shown in Table 2. The compositions represent discharge from LWR after two MOX recycles with minor actinides removed.

The edits requested of participants include the beginning-of-life eigenvalue and neutron balance, spectral indices and safety coefficients. Also requested are the composition and eigenvalue changes after a single burn cycle. Decay heat and isotopic contributions to toxicity (using toxicity factors specified in Table 3) are also requested.

Results

Six solutions were submitted for the oxide burner; Table 1 shows a synopsis of contributors, basic data and codes used in the solution of the problem. Some of the contributions were only partial.

In the following, we present an analysis of some major features of the exercise.

In Table 4, k-effective and critical balance are shown. In Tables 5, 6, and 7, neutron productions, absorptions (normalised to 1), and spectral indices at core centre are given.

A very large spread (almost 3%) can be observed in k-effective. Differences between the ANL solution and the PNC and PSI ones seem to be related to the difference in the leakage component of the critical balance and, therefore, the diffusion coefficient would be one major contributor to explain such a large discrepancy. We have to keep in mind also that the oxide fuel Pu-burner configuration is a high-leakage system. With respect to a previous benchmark [1], this system has a core leakage of $\approx 27\%$ against 16%. Basic data differences should be taken into account for the discrepancies with the IPPE and CEA solutions, even if such differences do not appear evident when we examine the results shown in Tables 5, 6, and 7. A perturbation calculation will be very helpful for identifying the contributions to the discrepancies by isotope and cross-section type.

Reactivity worths for sodium void and Doppler coefficient are shown in Tables 8 and 9 for beginning-of-life and end-of-cycle configuration. A quite disturbing picture appears for the sodium void coefficient where more than a factor of two exists for the whole reactor voiding between the

extreme solutions (ANL and PNC on one side and PSI on the other side). A look at Table 10 indicates that the main discrepancy lies in the non-leakage component.

The ANL Doppler reactivity worth is substantially lower than the other solutions because of the reduced contribution of the fertile isotopes (U-238 and Pu-240) as it can be seen in Table 11.

The end-of-cycle values show similar trends in the reactivity worths.

In Table 12, transport effects are shown for the configuration at the beginning of life. Very large discrepancies are found for the k -effective values. The two extreme values (IPPE and Toshiba) have been obtained by Monte Carlo codes. Continuous energy to multigroup data effect is probably responsible for the differences. The other solutions have been obtained using S_n theory codes.

Transport effect is not an issue for the Doppler coefficient calculation, but can represent an almost 10% correction of the total worth in the case of sodium void reactivity (see PNC solutions).

Tables 13 and 14 show results for reactivity loss and isotopic composition variation due to burnup. PNC and ANL are at the two extremes with the difference of 0.7% of $\Delta k/k'$ over the all life (625 days of burnup). Slight difference exists in the fission products contributions except for the PSI solution, that has a much larger value (28.7%). Related to the lower reactivity loss is the Pu-239 consumption rate of the ANL solution. The CEA results present a quite high value for the buildup of Am-243 and curium isotopes. The rather small value for the PSI solution for the U-238 composition variation suggests a quite low capture cross-section for the JEF-2.2 data file. Again for all those parameters, a perturbation analysis would be very valuable in understanding the differences.

Decay heat, neutron sources and activities are shown in Table 15. Decay heat results appear to be in good agreement between PNC and IPPE, while ANL has definitely lower values. The discrepancies between PNC and ANL are quite surprising because they use essentially the same code (ORIGEN) and associated library for the fission yields. Because differences on cross-sections can hardly explain the discrepancies on the results, starting conditions (isotopic compositions at discharge) and possibly different options (constant flux or power during irradiation) are the cause of the inconsistency. The large spread on the neutron source results has a possible reason in the fact that ANL version of ORIGEN was modified to better take into account (α , n) neutron productions.

Activities follow the same trend as the decay heat except for the IPPE results, that are lower (possibly some missing isotope contributions?).

Radiotoxicities at 0- and 1-million-year cooling time are shown in Tables 16 and 17. Total radiotoxicities are in quite good agreement when one considers the current uncertainties associated with this parameter. The good agreement can be explained by the fact that the radiotoxicity factors (that probably carry most of the uncertainties) have been imposed equal for all solutions (see Table 3). The higher value at 0 cooling time for the CEA total radiotoxicity is to be related to the presence of the larger buildup of curium isotopes already noticed in the isotopic composition variation. In Tables 18 and 19, the ANL solution for radiotoxicity is presented in two forms. In Table 18, the conventional method is utilised where the final density of the isotopes at the cooling time indicated is used to calculate the radiotoxicity. Table 19 gives, as required by the original benchmark proposal, the radiotoxicity on the whole descendance of subsequent daughters for a given initial nuclide. This definition allows to better understand the contribution of the initial isotopic composition to the total radiotoxicity.

Finally, in Table 20, the ANL solution is calculated using the radiotoxicity factors provided for the metallic fuel benchmark problem, which are shown in Table 21. This is done to allow a direct comparison of radiotoxicities expressed using the two different sets of toxicity conversion factors (Table 21 vs. Table 3) specified for the beginning-of-life benchmarks – the oxide and the metallic fuelled ones. In doing that, one has to bear in mind that initial mass inventory of the oxide and metal cores are different and the hypotheses on reprocessing losses are also different (0.1% of minor actinides for the metallic fuel and 0.3% of Pu and 1% of minor actinides for the oxide fuel).

To summarise the results provided by different organisations on the oxide fuel benchmark Pu-burner configuration, they show that an unsatisfactory situation is present for such fundamental parameters like k-effective and reactivity worths. Compared with previous benchmarks [1] [2], the picture is significantly worse. Even given that the configuration is a high leakage system, it would be very hard to accept so large a discrepancy. Only partial conclusions can be drawn at the present regarding the underlying causes of the poor agreements, and a perturbation analysis would be very useful in better understanding the differences in the results.

A more comfortable situation exists for radiotoxicities, where, given the status of the associated uncertainties, one would have expected larger discrepancies.

Further and deeper studies are surely needed. Experimental information, such as the ones coming from mock-up assemblies, would be necessary in the case that one day such a system is adopted for the design of a real power reactor.

Beginning-of-life metal-fuelled fast burner

Specification

The detailed metal-fuelled beginning-of-life benchmark specification is provided in Appendix B; only its main features are described here.

The benchmark design is a metal-fuelled burner core based on a 600-MWe (1575 MWth) configuration originally developed for low sodium void worth benchmark comparisons [3]. The cycle length is one year with an 85% capacity factor. One third of the core is refuelled per cycle. As shown in Figure 2, the core region is annular and contains 420 driver assemblies and 30 control subassemblies surrounding a (37 assembly) central reflector/absorber island. The driver active core height is only 45 cm (17.7 in.), roughly half the height of conventional fast reactor designs. This pancaked, annular geometry greatly enhances neutron leakage giving a low conversion ratio of roughly 0.5.

The axial design allocates a 15-cm reflector region directly below the core followed by a 30-cm shield region. The fuel pins extend above the active core region with a 70-cm fission gas plenum. Non-fuelled assemblies use a single composition over the entire axial height. The innermost three rows of the configuration shown in Figure 2 contain stainless steel assemblies, and the fourth row contains absorber (boron carbide) assemblies. Three rows of radial shielding surround the active core, a single row of steel and two rows of absorber. The material compositions of all fuelled and non-fuelled regions are specified in Table 22; the core composition is based on an estimate of beginning-of-life composition. For the start-up core, the fresh fuel is composed of recovered LWR transuranics (isotopic mix shown in Table 23) and depleted uranium.

A detailed analysis of the beginning-of-life neutron balance was requested of participants. Calculational results include: beginning-of-life eigenvalue, neutron flux energy spectrum, fission/absorption ratio, leakage/absorption ratio, capture/absorption ratio, and one-group collapsed cross-sections for the transuranic isotopes. Depletion results include the eigenvalue change and mass increments for a single cycle of depletion.

In addition to mass flow characteristics, the radiotoxicity of the fuel cycle inventories and discharged waste stream are evaluated in this benchmark. The mass flow results were converted to toxicity units using toxicity factors constructed using the methodology described by Bernard L. Cohen, [4] but using data from ICRP Publication 30, part 4, 1988 and BEIR III, 1980. These isotopic toxicity factors quantify the fatal cancer doses per gram ingested orally. They denote the hazard of the material rather than the risk because they do not include account of any pathway attenuation processes, but simply assume total oral ingestion. The specified toxicity factors are shown in Table 21; most important heavy metal and fission product isotopes are included.

Results

Four countries with five contributions participated in the beginning-of-cycle metal-fuelled benchmark. The list of participating countries, organisations, and authors is given in Table 1.

A brief review of the cross-section processing procedure, flux calculation, and depletion methodology applied by each of the participants is indicated below. Detailed information can be found in the contributed reports.

Europe [5]

The group constants originate from a 1968 group library based on JEF-2.2 data. Unit cell heterogeneity and slowing-down calculations were performed at the fine group level to generate a 33-group-cross-section set. This library was subsequently condensed to a 6-energy-group structure based on the regional flux distributions. Calculational results based on the CARNAVAL-IV data library were initially also submitted by the European team; however, problems were observed when this data was applied to metal fuel compositions, and only the JEF-2.2 based results are reported here.

The flux distribution was calculated using three-dimensional (Hex-Z) finite difference diffusion theory. Eigenvalue computations using other spatial methods (nodal diffusion and nodal transport theory) were also performed using the 33-group-cross-sections.

The depletion calculation was performed in three time steps, the time advance numerical method used is an exponential method. The capacity factor was included by derating the power level; thus, the power was normalised to 1335 MWth (85% of 1575 MWth). The flux level was normalised based on isotopic fission and capture energy production factors. Individual fission products are separately tracked in the calculation, although transmutation or migration of fission products during the cycle is not modelled.

Japan [6]

Two different cross sets were utilised: one based on JENDL-2 and the other on JENDL-3 data. For both sets, group constants were generated from a 70-group generic fast reactor library. This data was spatially collapsed to an 18-energy-group structure based on a two-dimensional (R-Z) flux calculation for the reference configuration.

The flux distribution was calculated using the CITATION code for a two-dimensional (R-Z) model using finite difference diffusion theory.

The depletion calculation was performed in five time steps using four radial and three axial zones, an additional depletion region was allocated for the core centre ring (giving a total of thirteen regional depletion zones for the fuel). The flux level was normalised using fission energy production factors which were corrected to account for capture reactions in the heavy nuclides; heating in the structural material was neglected. The fission products were modelled using four lumped fission products based on U-235, U-238, Pu-239, and Pu-241 fission.

Russia [7]

Group constants were generated from the ABBN-90 library which is based on FOND-2 data [8]. This 26-energy group data was regionally collapsed to 17- and 6-energy-group structures based on a three-dimensional (Hex-Z) calculation for the reference configuration.

The flux distribution was calculated using the TRIGEX code, nodal diffusion theory, for a three-dimensional (Hex-Z) model; nine axial layers are utilised in the core region.

The depletion calculation uses an analytical method to track the isotopic transmutations. The flux level was normalised based on isotopic fission and capture energy production factors. The fission products were modelled using two lumped fission products based on U-235 and Pu-239 fission.

United States [9]

Group constants were generated from the 2082-group MC²-2 library which is based on ENDF/B-V data. This data was collapsed to 230 energy groups based on an infinite-medium spectral calculation for a typical unit cell. This data was regionally collapsed to 21- and 9-energy-group structures based on a one-dimensional (R) flux calculation for the reference configuration.

The flux distribution was calculated using the DIF-3D code for a three-dimensional (Hex-Z) model. Nodal diffusion theory and the 9-group set were utilised for the depletion calculations; finite-difference diffusion theory and the 21-group set were utilised for the evaluation of reactivity feedbacks.

The depletion calculation was performed in a single time step using five radial and five axial (total of twenty-five) depletion zones for the fuel. The flux level was normalised using isotopic fission and capture energy production factors. The fission products were modelled using ten lumped fission products based on separated rare earth and non-rare earth components resulting from the fission of five different isotopes: U-235, U-238, Pu-239, Pu-240, and Pu-241.

Comparison of results

In the intercomparison of results, emphasis was placed on the neutron balance and on the eventual radiotoxicity of end-of-cycle discharged fuel. Results are compared at the beginning-of-life where the geometry and concentration was specified and variability can arise only from data and methods and also for the end-of-cycle case – depleted for one year at an 85% capacity factor where depletion methodology, flux normalisation, and fission product treatment can further add to discrepancies.

The neutronic performance characteristics are summarised in Table 24. The Russian and United States evaluations, which use nodal diffusion theory, show virtually identical eigenvalue predictions (0.1% difference at beginning-of-life, and 0.2% at end-of-cycle). The Japanese results (using R-Z finite difference diffusion theory) exhibit a 0.5% lower eigenvalue for JENDL-3 data compared with JENDL-2; including the mesh-size effect, the resulting eigenvalue prediction is 1.5% lower than the Russian and United States predictions. The European diffusion theory results are considerably (2-3%) lower than the other evaluations for both finite difference and nodal methods; the predicted eigenvalue was 2.2% higher when nodal transport theory was used. The neutron balance components in Table 24 show that the lower eigenvalue predictions in the European results are caused by a higher leakage fraction (the core leakage to absorption ratio is 0.623 as compared with 0.585 - 0.616 in the other evaluations). The fission and capture ratios are virtually identical between the evaluations; thus, the eigenvalue differences between the diffusion results are likely caused by discrepancies in the diffusion coefficient (transport cross-section). It is not surprising since implementation of the transport correction and methodology for diffusion coefficient prescription is where significant variations in group constant generation methods have historically been expected.

In summary, beginning-of-life eigenvalue predictions range from 1.063 to 1.102; significant differences are observed between nodal diffusion and nodal transport predictions (1.5%) and the transport effect is quite large (>2% eigenvalue effect) for this high leakage configuration. However, beginning-of-life eigenvalue, neutron balance, and burnup swing predictions are in reasonably close agreement for the Japanese (JENDL-3), Russian, and United States evaluations.

The transuranic isotope capture and fission one-group cross-sections (computed for the central core region) are summarised in Table 25. The multigroup collapsing spectra computed for this region are shown in Figure 3; these spectra appear to be consistent although large variations in the energy-group width are evident between participants. In Table 25, the 1σ variance of the reported effective one group cross-section values is used to indicate the spread in this result; this value does **not** indicate the expected uncertainty of the individual data. Fairly good agreement is observed for the fission cross-section results with variances of less than 5% for nearly all isotopes. The only large differences in the fission data are significantly higher Am-242m fission cross-sections in the Russian and United States evaluations, and significantly lower Cm-242 and Cm-243 fission cross-sections in the United States result. However, much larger variations are observed in the one-group capture data; as an example, the Am-243 capture cross-section ranges from 0.48 to 0.97 barns. This is understandable since little experimental *capture* data is available, particularly for the higher actinides, and much of the higher actinide data in modern evaluations is based on nuclear models. Better agreement is observed for the major transuranics (e.g., Pu-239 only ranges from 0.22-0.27 barns) where experimental data has been incorporated. Significant differences are observed between the JENDL-2 and JENDL-3 Japanese evaluations for several of the higher actinides (Am-241, Am-243, Cm-242, and Cm-243 in particular). These changes indicate a specific effort to improve the higher actinide data in the more recent JENDL-3 evaluation; and the magnitude of these changes (e.g., Cm-242 fission increases from 0.63 to 0.84 barns) is indicative of the large uncertainties which are present in current minor actinide data evaluations.

The beginning-of-life and end-of-cycle actinide masses are compared in Table 26; mass differences for isotopes ranging from U-234 to Cm-246 are shown. For most isotopes, the end-of-cycle mass is composed primarily of remaining beginning-of-life material; thus, only small percentage variations in the absolute end-of-cycle masses are observed. Thus, comparisons of the mass changes are more interesting. The total heavy metal loss rate ranges from -489 kg (Europe) to -509 kg (United States); this corresponds to energy production rates ranging from 1000 to 960 MWthd/kg, respectively. Significant differences in the mass change after one burn cycle are observed for individual isotopes; these differences are readily explained given the cross-section differences shown in Table 25. For example, the higher Pu-241 capture cross-sections in the European and Japanese results give more Pu-242 production in Table 26. In the European evaluation, the short-lived Am-242 (16 hour half-life) is explicitly modelled (note that Am-242 has been decayed into Cm-242 and Pu-242 for results in Table 26); this modelling change appears to yield a significantly higher Cm-242 end-of-cycle inventory of 8.28 kg as compared with roughly 4 kg in all other evaluations. Thus, a more detailed investigation of this branch of the decay chain is warranted.

The actinide mass values shown in Table 26 were converted to toxicity data using the toxicity factors shown in Table 21; results are summarised in Table 27. As shown in Table 27, the toxicity of the uranium inventory is much less than the toxicity of the transuranic inventory (by over seven orders of magnitude). As uranium decays over many thousands of years, the build-in of its daughters will cause the toxicity associated with this material to increase by roughly two orders of magnitude, but the resulting toxicity would still be less than any of the transuranic isotopes shown in Table 27. The total transuranic toxicity increases from 7.3E8 at beginning-of-life to 9.7E8 at end-of-cycle. This increase is primarily from the shorter-lived isotopes Cm-242 (+1.1E8), Cm-244 (+0.6E8), and Pu-238 (+0.6E8). The 6% variation in the end-of-cycle toxicity prediction is caused primarily by differences in the calculated end-of-cycle Cm-242 and Cm-244 inventories (see Table 26). Because Cm-242 and Cm-244 decay fairly rapidly (half-lives of 0.5 and 18 years, respectively), differences in their mass flow rates will not impact the long-term waste toxicity results.

In the 100-1,000 year timeframe, Am-241 will dominate the total toxicity. As shown in Table 27 with all Pu-241 decayed to Am-241, the total transuranic toxicity is 5.8E8, roughly half the end-of-cycle toxicity; the variation in this toxicity component between the various predictions is less than 0.5%.

In the 1,000-100,000 year timeframe, Pu-239 and Pu-240 will dominate the transuranic toxicity. The Pu-239 and Pu-240 toxicities sum to 8.9E7; and the variation between the predictions is less than 0.5%.

Finally, in the 100,000-1,000,000 year timeframe, Np-237 will dominate the total toxicity. As shown in Table 27 with all Pu-241 and Am-241 decayed to Np-237, the toxicity is 1.16E5; and the variation in the calculated results is quite small (~0.5%).

Given a specified initial composition and specified mass to toxicity conversion factors, the predicted toxicity of the spent fuel is seen to agree very well among participants even when reactor performance parameters do not. Some variation in the short-term toxicity (on the order of 6%) is observed because of differences in the predicted curium inventories; however, this difference decreases to less than 1% for the long-term toxicity predictions.

Conclusions

Six solutions were submitted for the oxide-fuelled beginning-of-life benchmark; five solutions were submitted for the metal-fuelled beginning-of-life benchmark as shown in Table 1. Tables 4 and 24 show eigenvalue and neutron balance results for the oxide and metal benchmarks, respectively. Variability of several percent Δk in predicted beginning-of-life eigenvalue for cores of specified geometry and composition is observed. While the Japanese, American, and Russian predictions are consistent for the metal core, a different pattern of clustering of participants' solutions is seen for the oxide core.

Tables 13 and 24 display the burnup reactivity loss for the oxide and metal cores, respectively; spreads of up to 1% $\Delta k/kk'$ out of a burnup swing of around 6% (metal), 8% (oxide) total reactivity loss are observed.

It is clear that for high leakage cores, two- and three-dimensional transport codes should be used; such codes are now available – but were not used by participants for this benchmark exercise. Their use could be expected to reduce the large variabilities in core leakage probability (see Tables 4 and 24) which are likely caused by methods' differences in generating diffusion coefficients. *Note that for the metal benchmark <1% eigenvalue errors exist upon transport corrections.*

Other than the above hypothesis, no broad characterisation of a principal cause of the large variabilities in predicting cores of specified geometry and composition has been found. It is hard to understand how participants who agree on beginning-of-life eigenvalue in one of the benchmarks disagree on the other. A followon effort to further wring out any misinterpretation of definitions and making use of transport solutions and of sensitivity coefficients of reactor parameters to cross-section library values would be useful.

Radiotoxicity flows relevant to the deployment of fast burner reactors as a waste management measure display less variability among participants than do operating and safety parameters – so long as consistent mass or curie-to-radiotoxicity conversion factors are employed. Tables 16 and 17 for oxide at discharge and at a-million-year cooling and Table 27 for metal at discharge illustrate this result.

Considering the large variabilities among participants' predictions of core performance, it is concluded that design and deployment of high leakage fast burner reactors will likely require supporting critical facility measurements to lower uncertainties in core operating and safety performance predictions. Alternately, the relatively less variability in predicted toxicity flows suggests that a second goal of the OECD/NEA Working Party benchmark exercise can lead already to useful characterisation of trends for fast reactor/thermal reactor symbiosis as a waste management measure. This is discussed in Volume 5.

References

- [1] L. G. Le Sage, R. D. McKnight, D. C. Wade, K. E. Freese and P. J. Collins, Proceedings of the NEACRP/IAEA Specialists Meeting on the International Comparison Calculation of a Large Sodium-Cooled Fast Breeder Reactor, Argonne National Laboratory, February 7-9, 1978, ANL-80-78, NEACRP-L-243 (1980).
- [2] G. Palmiotti and M. Salvatores, "NEACRP LMFBR Benchmark Calculation Intercomparison for Fuel Burnup", NEACRP-L-270 (1984).
- [3] R. N. Hill, M. Kawashima, K. Arie, and M. Suzuki, "Calculational Benchmark Comparisons for a Low Sodium Void Worth Actinide Burner Core Design", Proc. ANS Topical Meeting on Advances in Reactor Physics, Charleston, South Carolina, Vol. I, p. 313, March 8-11, 1992
- [4] B. L. Cohen, "Effects of ICRP Publication 30 and the 1980 BEIR Report on Hazard Assessments of High-Level Waste", Health Physics, 42, N°2, pp. 133-143 (1982).
- [5] G. Rimpault, J. Da Silva, and P. Smith, "European Neutronic Calculations for the Metal Fueled Fast Reactor Benchmark", Cadarache, April 1994.
- [6] S. Ohki and T. Yamamoto, "PNCs Results on the Metal-Fueled Fast Reactor Benchmarks", Power Reactor and Nuclear Fuel Development Corporation, August 1994.
- [7] A. Tsibulia, "Metal Fuel/Pyro Recycle", IPPE, Obninsk, July 1994.
- [8] A. I. Blokhin et al., "Current Status of Russian Evaluated Neutron Data Libraries", Proceedings of International Conference on Nuclear Data for Science and Technology, Gatlinburg, U.S.A., May 9-13 1994, vol. 2, p. 695.
- [9] K. N. Grimm, "Metallic-Fuel Benchmark Calculations", Argonne National Laboratory, October 1994.

Table 1
Participating countries and organisations for the OECD/NEA Fast Burner Physics Benchmarks

Oxide-fuelled fast burner benchmark

COUNTRY	ORGANISATION	CONTRIBUTORS	BASIC DATA	NUMBER OF ENERGY GROUP	CODES
<i>France</i>	CEA	J. C. Garnier F. Varaine	Carnaval-IV	25	HETAIRE, ERANOS
<i>Japan</i>	PNC	T. Ikegami T. Yamamoto S. Ohki	JENDL-2 JFS3-J2	18	SLAROM PERKY, TWO TRAN ORIGEN-2
<i>Japan</i>	TOSHIBA	M. Kawashima M. Yamaoka	JENDL-3 JFS-3, FSX	70	MCNP-3B
<i>Russia</i>	IPPE	A. M. Tsibulia	FOND-2 ABBN-90	26	SYNTES MMK CONSYST2 CARE
<i>Switzerland</i>	PSI	S. Pelloni	JEF-2.2	30	NJOY MICROR, MICROX-2 PSD, 2DTB ORIHET
<i>U.S.A.</i>	ANL	G. Palmiotti	ENDF/B-V	28	MC ² -2 SDX DIF3D REBUS VARI3D NUTS TWO DANT, ORIGEN-RA

BOL metal-fuelled fast burner benchmark

COUNTRY	ORGANISATION	CONTRIBUTORS	BASIC DATA	NUMBER OF ENERGY GROUP	FLUX SOLUTION
<i>European</i>	CEA-France AEA-UK	G. Rimpault, & J. Da Silva - CEA P. Smith - AEA	JEF-2.2	33	HEX-Z Finite Diff.
<i>Japan</i>	PNC	S. Ohki & T. Yamamoto	JFS-3-J2 (from JENDL-2) <hr/> JENDL-3	70 → 18 <hr/> 70 → 18	RZ Finite Diff.
<i>Russia</i>	IPPE	A. Tsibulia	ABBN-90 (from FOND-2)	26 → { 17 6	HEX-Z Nodal
<i>U.S.A.</i>	ANL	K. Grimm & R. Hill	ENDF/B-V	2082 → 230 → { 21 9	HEX-Z Nodal

Table 2
Oxide cores: Atomic number densities

REGION	NUCLIDE	CELL CALCULATION INNER ZONE	CELL CALCULATION OUTER ZONE	HOMOGENISED ATOMIC DENSITY
<i>I N N E R C O R E</i>	U-235	3.268-E-05		9.409E-06
	U-238	1.304E-02		3.754E-03
	Pu-238	3.015E-04		8.683E-05
	Pu-239	2.097E-03		6.037E-04
	Pu-240	1.426E-03		4.105E-04
	Pu-241	6.913E-04		1.990E-04
	Pu-242	7.573E-04		2.180E-04
	Am-241	6.913E-05		1.990E-05
	Fe		1.728E-02	1.231E-02
	Cr		4.973E-03	3.541E-03
	Ni		3.627E-03	2.583E-03
	Mo		4.360E-04	3.105E-04
	O	3.672E-02		1.057E-02
	Na		1.038E-02*	7.389E-03
	Mn		4.153E-04	2.957E-04
<i>O U T E R C O R E</i>	U-235	2.743E-05		7.899E-06
	U-238	1.095E-02		3.152E-03
	Pu-238	4.247E-04		1.223E-04
	Pu-239	2.953E-03		8.503E-04
	Pu-240	2.008E-03		5.782E-04
	Pu-241	9.736E-05		2.803E-04
	Pu-242	1.067E-03		3.071E-04
	Am-241	9.736E-05		2.803E-05
	Fe		1.728E-02	1.231E-02
	Cr		4.973E-03	3.541E-03
	Ni		3.627E-03	2.583E-03
	Mo		4.360E-04	3.105E-04
	O	3.684E-02		1.061E-02
	Na		1.038E-02*	7.389E-03
	Mn		4.153E-04	2.957E-04
<i>A X I A L A N D R A D I A L S H I E L D I N G</i>	Fe			2.662E-02
	Cr			7.662E-03
	Ni			5.588E-03
	Mo			6.717E-04
	Na			1.093E-02
	Mn			6.398E-04
<i>R O D F O L L O W E R</i>	Fe			7.987E-03
	Cr			2.299E-03
	Ni			1.676E-03
	Mo			2.015E-04
	Na			1.863E-02
	Mn			1.920E-04

* 0. for the voided cell. See section **Beginning-of-cycle oxide-fuelled fast burner, Specification**, on page 12.

Table 3
Hazard ingestion factors for oxide benchmark

NUCLIDE	HAZARD INGESTION FACTOR (Sv.Bq ⁻¹)
<i>Ac-227+</i>	3.9 E-6
<i>Am-241</i>	1.20 E-6
<i>Am-242m+</i>	1.14 E-6
<i>Am-243+</i>	1.19 E-6
<i>Cm-242</i>	3.54E-8
<i>Cm-243</i>	7.86 E-7
<i>Cm-244</i>	6.00 E-7
<i>Cm-245</i>	1.20 E-6
<i>Cm-246</i>	1.19 E-6
<i>Cm-247+</i>	1.11 E-6
<i>Cm-248</i>	4.40 E-6
<i>Np-237+</i>	1.06 E-6
<i>Pa-231</i>	2.89 E-6
<i>Pb-210+</i>	1.36 E-6
<i>Pu-236</i>	3.93 E-7
<i>Pu-238</i>	1.00 E-6
<i>Pu-239+</i>	1.16 E-6
<i>Pu-240</i>	1.16 E-6
<i>Pu-241+</i>	2.36 E-8
<i>Pu-242</i>	1.10 E-6
<i>Pu-244+</i>	1.08 E-6

NUCLIDE	HAZARD INGESTION FACTOR (Sv.Bq ⁻¹)
<i>Ra-226+</i>	3.05 E-7
<i>Ra-228</i>	3.40 E-7
<i>Th-228+</i>	2.00 E-7
<i>Th-229+</i>	1.05 E-6
<i>Th-230</i>	1.45 E-7
<i>Th-232</i>	7.40 E-7
<i>U-232</i>	3.44 E-7
<i>U-233</i>	7.20 E-8
<i>U-234</i>	7.20 E-8
<i>U-235+</i>	6.80 E-8
<i>U-236</i>	6.70 E-8
<i>U-238+</i>	6.70 E-8
<i>Tc-99</i>	3.4 E-10
<i>I-129</i>	7.4 E-8
<i>Cs-135</i>	1.9 E-9

+ indicates that the contribution of the short-life descendants is included.

Table 4
k-eff and critical balance at beginning of life

ORGANISATION	K-EFFECTIVE	ABSORPTION (%)	LEAKAGE (%)
ANL	1.10660	89.8	10.2
CEA	1.11170	89.0	11.0
PNC (J2)	1.12328	91.5	8.5
PNC (J3.2)	1.13106	91.0	9.0
Toshiba (J2)	1.11890	-	-
Toshiba (J3.1)	1.13488	-	-
PSI	1.12810	92.0	8.0
IPPE	1.11480	88.5	11.5

Table 5
Neutron productions at beginning of life normalised to 1.0

ISOTOPE	ANL	CEA	PNC (J2)	PNC (J3.2)	PSI	IPPE
U-235	0.0057	0.007	0.0060	0.0058	0.0058	0.0058
U-238	0.0657	0.075	0.0660	0.0655	0.0650	0.0665
Pu-238	0.0497	0.049	0.0475	0.0484	0.0476	0.0484
Pu-239	0.5231	0.522	0.5260	0.5237	0.5250	0.5254
Pu-240	0.0835	0.074	0.0795	0.0802	0.0800	0.0828
Pu-241	0.2361	0.243	0.2412	0.2422	0.2421	0.2384
Pu-242	0.0325	0.027	0.0302	0.0308	0.0305	0.0295
Am-241	0.0037	0.003	0.0036	0.0034	0.0034	0.0035
TOTAL	1.0000	1.000	1.0000	1.0000	1.0000	1.0000

Table 6
Absorptions at beginning of life normalised to 1.0

ISOTOPE	ANL	PNC (J2)	PNC (J3.2)	PSI	IPPE
<i>U-235</i>	0.0037	0.0394	0.0385	0.0037	0.0038
<i>U-238</i>	0.2139	0.2072	0.2096	0.2027	0.2096
<i>Pu-238</i>	0.0326	0.0349	0.0327	0.0290	0.0300
<i>Pu-239</i>	0.2786	0.2909	0.2916	0.2835	0.2890
<i>Pu-240</i>	0.0778	0.0802	0.0838	0.0674	0.0788
<i>Pu-241</i>	0.1155	0.1221	0.1237	0.1224	0.1174
<i>Pu-242</i>	0.0312	0.0034	0.0034	0.0325	0.0317
<i>Am-241</i>	0.0080	0.0090	0.0085	0.0087	0.0084
<i>O</i>	0.0018	0.0019	0.0016	0.0030	0.0027
<i>Fe</i>	0.0746	0.0877	0.0925	<i>STRUCTURAL MATERIALS PLUS SODIUM</i>	0.0800
<i>Cr</i>	0.0379	0.0298	0.0263		0.0300
<i>Ni</i>	0.0358	0.0409	0.0378		0.0381
<i>Mo</i>	0.0478	0.0507	0.0547		0.0490
<i>Mn</i>	0.0330	0.0297	0.0230		0.0237
<i>Na</i>	0.0078	0.0076	0.0069		0.0076
<i>TOTAL</i>	1.0000	1.0000	1.0000		1.0000

Table 7
Spectrum indexes at core center beginning of life

ORGANISATION	C238/F239	F238/F239	F240/F239	F241/F239
<i>ANL</i>	0.164	0.0265	0.229	1.351
<i>CEA</i>	0.16	0.03	0.21	1.36
<i>PNC (J2)</i>	0.154	0.027	0.217	1.376
<i>PNC (J3.2)</i>	0.154	0.027	0.221	1.390
<i>PSI</i>	0.154	0.0265	0.221	1.58
<i>IPPE</i>	0.157	0.0266	0.224	1.356

*Table 8
Reactivity worths at beginning of life (in % of $\Delta k/kk'$)*

ORGANISATION	SODIUM VOID INNER CORE	SODIUM VOID WHOLE CORE	DOPPLER
<i>ANL</i>	1.49	1.55	0.44
<i>CEA</i>	1.11	0.94	0.60
<i>PNC (J2)</i>	1.45	1.51	0.58
<i>PCN (J3.2)</i>	1.31	1.33	0.61
<i>Toshiba (J2)</i>	-	1.20	-
<i>Toshiba (J3.2)</i>	1.10	1.02	-
<i>PSI</i>	0.95	0.68	0.69
<i>IPPE</i>	1.04	0.90	0.62

*Table 9
Reactivity worths at end of cycle (in % of $\Delta k/kk'$)*

ORGANISATION	SODIUM VOID INNER CORE	SODIUM VOID WHOLE CORE	DOPPLER
<i>ANL</i>	1.85	2.01	0.461
<i>CEA</i>	1.41	1.30	0.642
<i>PNC (J2)</i>	1.81	1.97	0.609
<i>PNC (J3.2)</i>	1.64	1.73	0.633
<i>PSI</i>	1.25	1.02	0.709
<i>IPPE</i>	1.15	1.02	-

*Table 10
Beginning-of-life whole reaction sodium void reactivity worth by component*

	ANL	CEA	PNC (J2)	PNC (J3.2)	PSI
<i>NON LEAKAGE COMPONENT</i>	2.785	2.484	2.91	2.68	1.994
<i>LEAKAGE COMPONENT</i>	-1.235	-1.540	-1.40	-1.35	-1.318
<i>TOTAL</i>	1.550	0.944	1.51	1.33	0.676

*Table 11
Beginning-of-life Doppler reactivity worth by isotope component*

ISOTOPE	ANL	CEA	PNC (J2)	PNC (J3.2)	PSI	IPPE
U-238	0.393	0.586	0.450	0.503	0.621	0.527
Pu-239	-0.009	-0.057	-0.013	-0.009	-0.011	-0.004
Pu-240	0.026	0.066	0.043	0.052	0.053	0.067
Pu-241	0	-0.008	-0.002	-0.003	-0.004	-0.008
Pu-242	0.009	0	0.011	0.016	-	0.020
OTHERS	0.016	0.011	0.092	0.047	0.030	0.020
TOTAL	0.435	0.597	0.581	0.575	0.689	0.622

*Table 12
Transport effects at beginning of life(in % of $\Delta k/kk'$)*

ORGANISATION	K-EFFECTIVE	SODIUM VOID WHOLE CORE	DOPPLER
ANL	0.531	0.117	-0.002
PNC (J2)	0.525	0.148	-0.007
PNC (J3.2)	0.526	0.139	-0.004
Toshiba (J2)	-	0.180	-
Toshiba (J3.2)	-	0.029	-
PSI	0.285	0.003	-0.002
IPPE	0.734	-	-

*Table 13
Reactivity loss (in % of $\Delta k/kk'$)
(In parenthesis fission products contribution)*

ORGANISATION	BOL - EOC		BOL - EOL	
ANL	7.61	(20.5%)	12.85	(20.1%)
CEA	7.90	(20.3%)	13.27	
PNC (J2)	8.03	(23.1%)	13.60	(25.0%)
PNC (J3.2)	7.91	(23.5%)	13.39	(25.2%)
PSI	7.79	(27.6%)	13.06	(28.7%)

Table 14
Isotopic composition variation EOL - BOL (Δ kg)

ISOTOPE	ANL	CEA	PNC (J2)	PNC (J3.2)	PSI
U-235	-5.6	-5.9	-5.8	-5.7	-5.5
U-238	-420	-411	-392	-390	-384
Pu-238	-50	-45	-50	-47	-43.4
Pu-239	-149	-174	-170	-131	-173
Pu-240	-38	-21	-32	-13	-34
Pu-241	-133	-139	-133	-122	-137
Pu-242	-29	-42	-31	-20	-25
Am-241	9.1	7.5	8.3	9.5	8.6
Am-243	31	44	33	34	33
Cm-242	3.7	5.2	4.8	4.5	4.1
Cm-244	4.1	7.4	5.3	5.3	5.4

Table 15
Decay heat, neutron sources and activities at different cooling times

			ANL	PNC (J2)	PNC (J3.2)	IPPE
DECAY HEAT	(W)	IC	2.37 E + 4	2.93 E + 4	2.93 E + 4	2.80 E + 4
COOLING TIME	(1 DAY)	OC	2.07 E + 4	2.79 E + 4	2.79 E + 2	2.40 E + 4
DECAY HEAT	(W)	IC	1.62 E + 3	2.05 E + 3	2.05 E + 3	2.00 E + 4
COOLING TIME	(1 YEAR)	OC	1.67 E + 3	2.27 E + 3	2.27 E + 3	2.07 E + 3
NEUTRON SOURCE	(n/sec)	IC	9.77 E + 8	5.91 E + 8	5.91 E + 8	7.21 E + 8
COOLING TIME	(1 DAY)	OC	9.41 E + 8	6.40 E + 8	6.39 E + 8	6.52 E + 8
NEUTRON SOURCE	(n/sec)	IC	3.28 E + 8	2.72 E + 8	2.71 E + 8	3.65 E + 8
COOLING TIME	(1 YEAR)	OC	3.27 E + 8	2.68 E + 8	2.67 E + 8	2.78 E + 8
ACTIVITY	(Bq)	IC	2.35 E + 17	2.64 E + 17	2.64 E + 17	1.84 E + 17
COOLING TIME	(1 DAY)	OC	1.94 E + 17	2.41 E + 17	2.40 E + 17	1.65 E + 17
ACTIVITY	(Bq)	IC	1.29 E + 16	1.59 E + 16	1.59 E + 16	1.16 E + 16
COOLING TIME	(1 YEAR)	OC	1.43 E + 16	1.81 E + 16	1.81 E + 16	1.05 E + 16

Table 16
Radiotoxicities Cooling time 0

ISOTOPE	ANL	PNC	CEA
Am-241	7.69 E + 7	7.75 E + 7	7.48 E + 7
Am-242m	8.58 E + 6	8.65 E + 6	7.79 E + 6
Am-243	2.75 E + 6	2.70 E + 6	3.83 E + 6
Cm-242	1.62 E + 8	1.61 E + 6	2.07 E + 8
Cm-243	1.95 E + 6	1.74 E + 6	4.50 E + 6
Cm-244	7.33 E + 7	5.15 E + 4	1.33 E + 8
Cm-245	1.69 E + 4	1.03 E + 4	2.29 E + 4
Pu-238	2.44 E + 8	2.44 E + 8	2.56 E + 8
Pu-239	8.80 E + 6	8.60 E + 6	8.59 E + 6
Pu-240	2.39 E + 7	2.39 E + 7	2.44 E + 7
Pu-241	7.48 E + 7	7.50 E + 7	7.32 E + 7
Pu-242	2.05 E + 5	1.99 E + 5	1.99 E + 5
Tc-99	3.55 E + 3	3.64 E + 3	-
I-129	2.35 E + 3	2.69 E + 3	-
Cs-135	2.36 E + 3	2.40 E + 3	-
TOTAL	6.77 E + 8	6.55 E + 8	7.90 E + 8

Table 17
Radiotoxicities Cooling time 1 E + 6 Years

ISOTOPE	ANL	PNC	CEA	PSI
Ac-227	1.11 E + 3	1.10 E + 3	1.14 E + 3	1.13 E + 3
Np-237	2.70 E + 4	2.68 E + 4	2.65 E + 4	2.91 E + 4
Pa-231	8.20 E + 2	8.15 E + 2	8.43 E + 2	8.38 E + 2
Pb-210	1.17 E + 4	1.17 E + 4	1.28 E + 4	1.35 E + 4
Pu-242	3.26 E + 4	3.33 E + 4	- ^{a)}	3.37 E + 4
Ra-226	2.63 E + 3	2.62 E + 3	2.88 E + 3	3.03 E + 3
Th-229	3.71 E + 4	2.82 E + 4	2.79 E + 4	3.06 E + 4
Th-230	1.24 E + 3	1.25 E + 4	1.36 E + 3	1.44 E + 3
U-233	1.95 E + 3	1.94 E + 3	- ^{a)}	2.10 E + 3
U-234	4.24 E + 2	4.23 E + 2	- ^{a)}	4.81 E + 2
U-235	1.93 E + 1	1.92 E + 1	- ^{a)}	1.92 E + 1
U-236	3.81 E + 2	3.78 E + 2	- ^{a)}	3.87 E + 2
Tc-99	1.37 E + 2	1.41 E + 2	-	8.37 E + 1
I-129	2.25 E + 3	2.57 E + 3	-	1.45 E + 3
Cs-135	1.74 E + 3	1.78 E + 3	-	1.11 E + 3
TOTAL	1.21 E + 5	1.13 E + 5	- ^{a)}	1.20 E + 5

a) CEA took into account an extra 0.3% of U as a loss. This will affect the comparison for this isotope.

Table 18
Radiotoxicity (Sv) for the ANL solution standard method

ISOTOPE	0 Y	100 Y	1000 Y	10000 Y	100000 Y	100000 Y
Ac-227	0	1.73 E-3	2.85 E-1	2.66 E+1	7.69 E+2	1.11 E+3
Am-241	7.69 E+7	1.78 E+8	4.25 E+7	7.90 E+3	5.03 E+0	0
Am-242m	8.58 E+6	5.44 E+6	9.01 E+4	0	0	0
Am-243	2.75 E+6	2.73 E+6	2.51 E+6	1.08 E+6	2.31 E+2	0
Cm-242	1.62 E+8	1.39 E+5	2.31 E+3	0	0	0
Cm-243	1.95 E+6	1.71 E+5	5.44 E-5	0	0	0
Cm-244	7.33 E+7	1.60 E+6	1.78 E-9	0	0	0
Cm-245	1.69 E+4	1.68 E+6	1.56 E+4	7.46 E+3	4.76 E+0	0
Cm-246	5.43 E+2	5.35 E+2	4.69 E+2	1.26 E+2	2.38 E-4	0
Np-237	4.75 E+2	5.24 E+3	2.97 E+4	3.72 E+4	3.62 E+4	2.70 E+4
Pa-231	0	2.28 E-3	2.25 E-1	1.98 E+1	5.70 E+2	8.20 E+2
Pb-210	0	2.63 E-1	1.67 E+2	8.79 E+3	6.79 E+4	1.17 E+4
Pu-236	1.74 E+2	4.81 E-9	0	0	0	0
Pu-238	2.44 E+8	1.24 E+8	2.49 E+5	0	0	0
Pu-239	8.80 E+6	8.78 E+6	8.62 E+6	7.03 E+6	5.65 E+5	3.34 E-6
Pu-240	2.39 E+7	2.40 E+7	2.18 E+7	8.43 E+6	6.20 E+2	0
Pu-241	7.48 E+7	6.72 E+5	3.07 E+2	1.47 E+2	9.38 E-2	0
Pu-242	2.05 E+5	2.05 E+5	2.05 E+5	2.02 E+5	1.71 E+5	3.26 E+4
Ra-226	0	1.23 E-1	4.00 E+1	1.98 E+3	1.52 E+4	2.63 E+3
Ra-228	0	4.37 E-8	4.94 E-6	3.77 E-4	8.91 E-3	9.62 E-2
Th-228	0	1.44 E+0	1.97 E-4	2.21 E-4	5.24 E-3	5.66 E-2
Th-229	0	3.82 E-3	2.76 E+0	5.35 E+2	1.48 E+4	3.71 E+4
Th-230	0	3.88 E+0	1.12 E+2	1.21 E+3	7.32 E+3	1.24 E+3
Th-232	0	1.12 E-7	1.09 E-5	8.21 E-4	1.94 E-2	2.09 E-1
U-232	0	2.40 E+0	3.24 E-4	0	0	0
U-233	0	8.02 E-2	5.52 E+0	1.02 E+2	8.81 E+2	1.95 E-3
U-234	0	3.80 E+3	7.16 E+3	6.98 E+3	5.41 E+3	4.24 E+2
U-235	0	5.07 E-2	5.02 E-1	4.56 E+0	1.82 E+1	1.93 E+1
U-236	0	4.11 E+0	3.93 E+1	2.56 E+2	3.91 E+2	3.81 E+2
U-238	0	1.93 E-4	1.93 E-3	1.92 E-2	1.77 E-1	8.86 E-1
Tc-99	3.55 E+3	3.55 E+3	3.54 E+3	3.44 E+3	2.57 E+3	1.37 E+2
I-129	2.35 E+3	2.35 E+3	2.35 E+3	2.35 E+3	2.34 E+3	2.25 E+3
Cs-135	2.36 E+3	2.36 E+3	2.35 E+3	2.35 E+3	2.29 E+3	1.74 E+3
TOTAL	6.77 E+8	3.46 E+8	7.60 E+7	1.68 E+7	8.93 E+5	1.21 E+5

Table 19
Radiotoxicity (Sv) for the ANL solution whole descendance is included for each isotope

ISOTOPE	0 Y	100 Y	1000 Y	10000 Y	100000 Y	1000000 Y
Am-241	0	1.42 E-6	1.55 E+7	1.39 E+3	1.91 E+4	2.43 E+4
Am-242m	8.58 E+6	8.23 E+6	2.43 E+5	1.29 E+3	4.90 E+3	7.14 E+2
Am-243	2.75 E+6	2.74 E+6	2.58 E+6	1.50 E+6	6.72 E+4	1.03 E+2
Cm-242	1.62 E+8	1.06 E+7	9.35 E+3	1.59 E+3	8.02 E+3	1.34 E+3
Cm-243	1.95 E+6	1.75 E+5	3.33 E+3	2.56 E+3	1.93 E+2	4.27 E-1
Cm-244	7.33 E+7	1.98 E+6	3.53 E+5	1.37 E+5	6.41 E+2	6.14 E+2
Cm-245	1.69 E+4	1.91 E+4	2.86 E+4	1.55 E+4	8.91 E+1	1.05 E+3
Cm-246	5.43 E+2	5.34 E+2	4.70 E+2	1.30 E+2	5.31 E+0	1.02 E+0
Np-237	4.76 E+2	4.76 E+2	4.76 E+2	4.83 E+2	6.61 E+2	8.41 E+2
Pu-238	2.44 E+8	1.11 E+8	9.76 E+2	1.67 E+4	8.41 E+4	1.41 E+4
Pu-239	8.80 E+6	8.77 E+6	8.55 E+6	6.60 E+6	4.98 E+5	1.10 E+3
Pu-240	2.39 E+7	2.36 E+7	2.15 E+7	8.32 E+6	1.10 E+3	5.00 E+2
Pu-241	7.48 E+7	1.13 E+8	2.70 E+7	2.34 E+5	3.20 E+4	4.08 E+4
Pu-242	2.05 E+5	2.05 E+5	2.04 E+5	2.01 E+5	1.70 E+5	3.25 E+4
Tc-99	3.55 E+3	3.55 E+3	3.54 E+3	3.44 E+3	2.57 E+3	1.37 E+2
I-129	2.35 E+3	2.35 E+3	2.35 E+3	2.35 E+3	2.34 E+3	2.25 E+3
C-135	2.36 E+3	2.36 E+3	2.36 E+3	2.35 E+3	2.29 E+3	1.74 E+3
TOTAL	6.77 E+8	3.46 E+8	7.60 E+7	1.68 E+7	8.93 E+5	1.21 E+5

Table 20
Radiotoxicity calculated using factors specified in the metal fuel benchmark. ANL solution.

ISOTOPE	0 Y	100 Y	1000 Y	10000 Y	100000 Y	100000 Y
Ac-227	0	1.42 E-3	2.34 E-3	2.18 E-1	6.31 E+0	9.09 E+0
Am-241	4.73 E+5	1.10 E+6	2.61 E+5	4.85 E+1	3.09 E-2	0
Am-242m	5.44 E+4	3.45 E+4	5.71 E+2	0	0	0
Am-243	1.71 E+4	1.69 E+4	1.55 E+4	6.68 E+3	1.43 E+0	0
Cm-242	8.54 E+4	7.35 E+2	1.22 E+1	0	0	0
Cm-243	1.32 E+4	1.16 E+3	3.68 E-7	0	0	0
Cm-244	5.38 E+5	1.17 E+4	0	0	0	0
Cm-245	1.09 E+2	1.08 E+0	1.00 E+2	4.81 E+1	3.07 E-2	0
Cm-246	3.50 E+0	3.45 E+0	3.02 E+0	8.10 E-1	1.54 E-6	0
Np-237	2.39 E+0	2.63 E+1	1.49 E+2	1.87E+1	1.82 E+2	1.36 E+2
Pa-231	0	7.92 E-6	7.82 E-4	6.89 E-2	1.98 E+0	2.85 E+0
Pb-210	0	2.38 E-3	1.51 E+0	7.95 E+1	6.14 E+2	1.06 E+2
Pu-236	1.16 E+0	0	0	0	0	0
Pu-238	1.62 E+6	8.25 E+5	1.66 E+3	0	0	0
Pu-239	5.48 E+4	5.47 E+4	5.37 E+4	4.38 E+4	3.52 E+3	2.08 E-8
Pu-240	1.49 E+5	1.50 E+5	1.36 E+5	5.25 E+4	3.87 E+0	0
Pu-241	4.66 E+5	4.19 E+3	1.91 E+0	9.16 E-1	5.85 E-4	0
Pu-242	1.35 E+3	1.35 E+3	1.35 E+3	1.32 E+3	1.12 E+3	2.14 E+2
Ra-226	0	3.97 E-4	1.29 E-1	6.37 E+0	4.90 E+1	8.47 E+0
Ra-228	0	1.41 E-10	1.59 E-8	1.21 E-6	2.87 E-5	3.09 E-4
Th-228	0	4.71 E-3	6.44 E-7	7.25 E-7	1.72 E-5	1.85 E-4
Th-229	0	1.25 E-5	9.06 E-3	1.75 E+0	4.84 E+1	1.22 E+2
Th-230	0	1.38 E-2	3.99 E-1	4.32 E+0	2.61 E+1	4.43 E+0
Th-232	0	4.00 E-10	3.90 E-8	2.93 E-6	6.91 E-5	7.46 E-4
U-232	0	6.85 E-3	9.23 E-7	0	0	0
U-233	0	2.29 E-4	1.57 E-2	2.90 E-1	2.51 E+0	5.55 E+0
U-234	0	1.08 E+1	2.04 E+1	1.99 E+1	1.54 E+1	1.21 E+0
U-235	0	1.46 E-4	1.44 E-3	1.31 E-2	5.22 E-2	5.55 E-2
U-236	0	1.24 E-2	1.19 E-1	7.74 E-1	1.18 E+0	1.15 E+0
U-238	0	5.44 E-4	5.44 E-3	5.40 E-2	4.98 E-1	2.49 E+0
Tc-99	4.86 E+1	4.86 E+1	4.84 E+1	4.70 E+1	3.51 E+1	1.88 E+9
I-129	5.56 E+1	5.56 E+1	5.56 E+1	5.56 E+1	5.54 E+1	5.39 E+1
Cs-135	2.82 E+1	2.82 E+1	2.82 E+1	2.81 E+1	2.74 E+1	2.09 E+1
TOTAL	4.24 E+6	2.20 E+6	4.70 E+5	1.05 E+5	5.71 E+3	6.89 E+2

Table 21
Radiotoxicity data
(CD = Cancer Dose Hazard)

ISOTOPE	TOXICITY FACTOR CD/Ci	HALF-LIFE YEARS	TOXICITY FACTOR CD/g
Actinides and Their Daughters			
Pb-210	455.0	22.3	3.48E4
Ra-223	15.6	0.03	7.99E5
Ra-226	36.3	1.60E3	3.59E1
Ac-227	1185.0	21.8	8.58E4
Th-229	127.3	7.3E3	2.72E1
Th-230	19.1	7.54E4	3.94E-1
Pa-231	372.0	3.28E4	1.76E-1
U-234	7.59	2.46E5	4.71E-2
U-235	7.23	7.04E8	1.56E-5
U-236	7.50	2.34E7	4.85E-4
U-238	6.97	4.47E9	2.34E-6
Np-237	197.2	2.14E6	1.39E-1
Pu-238	246.1	87.7	4.22E3
Pu-239	267.5	2.41E4	1.66E1
Pu-240	267.5	6.56E3	6.08E1
Pu-242	267.5	3.75E5	1.65E0
Am-241	272.9	433	9.36E2
Am-242m	267.5	141	2.80E4
Am-243	272.9	7.37E3	5.45E1
Cm-242	6.90	0.45	2.29E4
Cm-243	196.9	29.1	9.96E3
Cm-244	163.0	18.1	1.32E4
Cm-245	284.0	8.5E3	4.88E1
Cm-246	284.0	4.8E3	8.67E1
Short-Lived Fission Products			
Sr-90	16.7	29.1	2.28E3
Y-90	0.60	7.3E-3	3.26E5
Cs-137	5.77	30.2	4.99E2
Long-Lived Fission Products			
Tc-99	0.17	2.13E5	2.28E-3
I-129	64.8	1.57E7	1.15E-2
Zr-93	0.095	1.5E6	2.44E-4
Cs-135	0.84	2.3E6	9.68E-4
C-14	0.20	5.73E3	8.92E-1
Ni-59	0.08	7.6E4	6.38E-3
Ni-63	0.03	100	1.70E0
Sn-126	1.70	1.0E5	4.83E-2

Table 22
Material composition specifications
(Number Densities in atoms/barn-cm)

ISOTOPE	DRIVER				CONTROL		EXCHANGE	REFLECTOR	SHIELD
	SHIELD	REFLECTOR	CORE	PLENUM	IN	OUT			
Na-23	7.447-3	7.447-3	7.637-3	1.678-2	8.865-3	2.080-2	6.075-3	3.546-3	3.546-3
Fe	1.179-2	4.821-2	1.790-2	1.790-2	1.538-2	4.865-3	1.405-2	6.088-2	1.516-2
Cr	1.761-3	7.201-3	2.674-3	2.674-3	2.297-3	7.265-4	2.100-3	9.092-3	2.263-3
Mo	7.952-5	3.252-4	1.207-4	1.207-4	1.038-4	3.281-5	9.485-5	4.106-4	1.022-4
Ni	6.499-5	2.658-4	9.868-5	9.868-5	8.479-5	2.681-5	7.751-5	3.356-4	8.354-5
Mn-55	2.777-5	1.136-4	4.217-5	4.217-5	3.624-5	1.146-5	3.313-5	1.434-4	3.570-5
B-10	9.278-3				2.783-2		8.017-3		9.495-3
B-11	3.758-2				3.092-3		3.247-2		3.845-2
C-12	1.171-2				7.731-3		1.012-2		1.199-2
Zr			3.189-3						
U-235			1.632-5						
U-238			8.144-3						
Np-237			1.521-4						
Pu-236			3.155-10						
Pu-238			2.845-5						
Pu-239			1.431-3						
Pu-240			5.606-4						
Pu-241			3.775-4						
Pu-242			1.093-4						
Am-241			7.071-5						
Am-242m			3.127-7						
Am-243			6.987-5						
Cm-242			2.741-8						
Cm-243			2.214-7						
Cm-244			1.555-5						
Cm-245			1.431-6						
Cm-246			1.778-7						

Table 23
LWR transuranic isotopics

Isotopic values are the weight fraction of the individual isotope in the total transuranic mass

LWR

ISOTOPE AT 3.17 YEARS COOLING

Np-237	5.40-2
Pu-236	1.12-7
Pu-238	1.01-2
Pu-239	0.508
Pu-240	0.199
Pu-241	0.134
Pu-242	3.88-2
Am-241	2.51-2
Am-242m	1.11-4
Am-243	2.48-2
Cm-242	9.73-6
Cm-243	7.86-5
Cm-244	5.52-3
Cm-245	5.08-4
Cm-246	6.31-5
MA/fiss. Pu	0.172
MA/Pu	0.124
Np-237/MA	0.490
Am-241/MA	0.228
Am-243/MA	0.225
Np-chain	0.213

MA = sum of minor actinides;
fiss. Pu = Pu-239 + Pu-241;
Np-chain = Np-237 + Am-241 + Pu-241.

Table 24
Comparison of reference core neutronic characteristics

	EUROPE	JAPAN JENDL-2	JAPAN JENDL-3	RUSSIA	UNITED STATES
<i>BOL EIGENVALUE</i>	1.063 ^{a)}	1.098	1.092 ^{b)}	1.102	1.101
<i>BOL NEUTRON BALANCE</i>					
Fissions per Core Absorption		0.589	0.592	0.600	0.599
HM Captures per Core Absorption		0.376	0.374	0.370	0.366
Structure Captures per Core Absorption		0.034	0.033	0.030	0.033
Coolant Captures per Core Absorption		0.001	0.001	0.001	0.001
Core Leakage per Core Absorption	0.623	0.585	0.601	0.616	0.612
Model Leakage per Model Absorption		0.026	0.027	0.014	0.030
EOL Eigenvalue	1.012	1.040	1.034	1.040	1.042
Burnup Swing, %Δk	-5.1	-5.8	-5.8	-6.2	-5.9
Transuranic Inventory Ratio (EOL/BOL)	0.944	0.944	0.944	0.943	0.944

^{a)} Eigenvalue using nodal diffusion and nodal transport theory are 1.078 and 1.100, respectively.

^{b)} Estimated eigenvalue with mesh corrections applied is 1.085.

Table 25
Comparison of one-group transuranic cross-sections

ISOTOPE	EUROPE	JAPAN JENDL-2	JAPAN JENDL-3	RUSSIA	UNITED STATES	MEAN VALUE	
Np-237	σ_f	0.47	0.43	0.43	0.47	0.48	$0.46 \pm 5\%$
	$\nu\sigma_f$	1.31	1.19	1.19	1.38	1.40	$1.29 \pm 7\%$
	σ_c	0.83	0.93	0.99	0.80	0.86	$0.88 \pm 8\%$
Pu-238	σ_f	1.23	1.21	1.19	1.21	1.21	$1.21 \pm 1\%$
	$\nu\sigma_f$	3.73	3.65	3.59	3.68	3.67	$3.66 \pm 1\%$
	σ_c	0.28	0.54	0.40	0.30	0.42	$0.39 \pm 24\%$
Pu-239	σ_f	1.63	1.68	1.64	1.63	1.65	$1.65 \pm 1\%$
	$\nu\sigma_f$	4.85	4.99	4.88	4.85	4.89	$4.89 \pm 1\%$
	σ_c	0.23	0.26	0.27	0.24	0.22	$0.24 \pm 8\%$
Pu-240	σ_f	0.52	0.48	0.46	0.49	0.50	$0.49 \pm 4\%$
	$\nu\sigma_f$	1.56	1.45	1.38	1.52	1.52	$1.49 \pm 4\%$
	σ_c	0.29	0.32	0.35	0.30	0.29	$0.31 \pm 7\%$
Pu-241	σ_f	1.93	2.01	2.03	1.95	1.92	$1.97 \pm 2\%$
	$\nu\sigma_f$	5.82	6.03	6.10	5.87	5.76	$5.92 \pm 2\%$
	σ_c	0.39	0.33	0.32	0.23	0.26	$0.31 \pm 18\%$
Pu-242	σ_f	0.39	0.36	0.34	0.35	0.38	$0.36 \pm 5\%$
	$\nu\sigma_f$	1.18	1.09	1.03	1.07	1.15	$1.10 \pm 5\%$
	σ_c	0.24	0.27	0.29	0.25	0.22	$0.25 \pm 10\%$
Am-241	σ_f	0.39	0.40	0.35	0.40	0.41	$0.39 \pm 5\%$
	$\nu\sigma_f$	1.41	1.40	1.22	1.37	1.38	$1.36 \pm 5\%$
	σ_c	1.20	1.23	1.09	1.04	1.01	$1.11 \pm 8\%$
Am-242m	σ_f	2.40	2.59	2.53	2.84	2.80	$2.63 \pm 6\%$
	$\nu\sigma_f$	7.87	8.68	8.46	9.46	9.37	$8.77 \pm 7\%$
	σ_c	0.34	0.30	0.38	0.16	0.15	$0.27 \pm 35\%$
Am-243	σ_f	0.31	0.32	0.25	0.32	0.33	$0.31 \pm 8\%$
	$\nu\sigma_f$	1.06	1.14	0.90	1.17	1.19	$1.09 \pm 10\%$
	σ_c	0.95	0.95	0.97	0.48	0.70	$0.81 \pm 24\%$
Cm-242	σ_f	0.77	0.63	0.84	0.90	0.23	$0.67 \pm 36\%$
	$\nu\sigma_f$	2.60	2.38	2.89	3.02	0.89	$2.36 \pm 33\%$
	σ_c	0.22	0.32	0.30	0.24	0.12	$0.24 \pm 29\%$
Cm-243	σ_f	2.57	2.78	2.41	--	2.01	$2.44 \pm 12\%$
	$\nu\sigma_f$	8.95	9.80	8.48	--	7.11	$8.59 \pm 11\%$
	σ_c	0.09	0.12	0.24	--	0.11	$0.14 \pm 42\%$
Cm-244	σ_f	0.61	0.55	0.52	0.58	0.58	$0.57 \pm 5\%$
	$\nu\sigma_f$	2.14	1.93	1.85	2.17	2.18	$2.05 \pm 7\%$
	σ_c	0.33	0.33	0.43	0.50	0.49	$0.42 \pm 18\%$
Cm-245	σ_f	2.06	2.23	2.16	2.20	2.18	$2.17 \pm 3\%$
	$\nu\sigma_f$	8.11	8.75	7.76	8.66	8.58	$8.37 \pm 5\%$
	σ_c	0.17	0.12	0.25	0.20	0.19	$0.19 \pm 23\%$
Cm-246	σ_f	--	0.36	0.34	0.42	0.39	$0.38 \pm 8\%$
	$\nu\sigma_f$	--	1.26	1.20	1.39	1.49	$1.34 \pm 8\%$
	σ_c	--	0.19	0.20	0.15	0.12	$0.17 \pm 19\%$

Table 26
Comparison of reference mass flow characteristics (all values in kg)

ISOTOPE	EUROPE	JAPAN JENDL-2	JAPAN JENDL-3	RUSSIA	UNITED STATES	MEAN VALUE
U-234 BOL	0.0	--	--	--	0.0	0.0
EOL	0.39	--	--	--	0.33	0.36 ± 8%
(EOL-BOL)	0.39	--	--	--	0.33	0.36 ± 8%
U-235 BOL	25.4	25.4	25.4	25.2	25.4	25.4
EOL	22.1	21.8	21.8	21.7	21.9	21.9 ± 0.6%
(EOL-BOL)	-3.3	-3.6	-3.6	-3.6	-3.5	-3.5 ± 3%
U-236 BOL	0.0	0.0	0.0	--	0.0	0.0
EOL	0.71	0.79	0.77	--	0.73	0.75 ± 4%
(EOL-BOL)	0.71	0.79	0.77	--	0.73	0.75 ± 4%
U-238 BOL	12,849	12,850	12,850	12,738	12,851	12,850
EOL	12,611	12,594	12,596	12,485	12,594	12,576 ± 0.4%
(EOL-BOL)	-238	-257	-254	-253	-257	-252 ± 2.8%
Np-237 BOL	239	239	239	237	239	239
EOL	215	215	214	214	215	215 ± 0.2%
(EOL-BOL)	-24.0	-23.6	-25.0	-23.1	-23.6	-23.9 ± 3%
Pu-238 BOL	44.9	44.9	44.9	44.5	44.9	44.9
EOL	55.8	59.5	59.6	58.0	58.6	58.3 ± 2%
(EOL-BOL)	10.9	14.6	14.7	13.5	13.2	13.4 ± 10%
Pu-239 BOL	2,267	2,268	2,268	2,248	2,268	2,268
EOL	2,118	2,117	2,118	2,098	2,125	2,115 ± 0.4%
(EOL-BOL)	-149	-150	-149	-150	-143	-148 ± 2%
Pu-240 BOL	892	892	892	884	892	892
EOL	884	887	883	876	880	882 ± 0.4%
(EOL-BOL)	-8.0	-5.3	-8.7	-7.9	-12.1	-8.4 ± 26%
Pu-241 BOL	603	603	603	598	603	603
EOL	496	499	500	494	502	498 ± 0.6%
(EOL-BOL)	-107	-104	-103	-103	-101	-104 ± 2%
Pu-242 BOL	175	175	175	174	175	175
EOL	186	183	182	178	181	182 ± 1%
(EOL-BOL)	11.0	7.8	8.3	4.0	5.2	7.3 ± 34%
Am-241 BOL	113	113	113	112	113	113
EOL	123	119	121	123	121	121 ± 1%
(EOL-BOL)	10.0	6.5	8.3	11.1	7.8	8.7 ± 19%
Am-242m BOL	0.50	0.50	0.50	0.50	0.50	0.50
EOL	1.61	2.58	2.29	1.94	2.22	2.13 ± 15%
(EOL-BOL)	1.11	2.08	1.79	1.44	1.72	1.63 ± 20%
Am-243 BOL	113	113	113	112	113	113
EOL	105	105	106	108	107	106 ± 1%
(EOL-BOL)	-8.0	-7.4	-6.7	-3.8	-5.9	-6.4 ± 23%

Table 26 (cont.)

ISOTOPE	EUROPE	JAPAN JENDL-2	JAPAN JENDL-3	RUSSIA	UNITED STATES	MEAN VALUE
Cm-242 BOL	0.04	0.04	0.04	0.04	0.04	0.04
EOL	8.28	4.54	3.93	3.82	3.82	4.88 ± 35%
(EOL-BOL)	8.24	4.50	3.88	3.78	3.77	4.83 ± 36%
Cm-243 BOL	0.36	0.36	0.36	--	0.35	0.36
EOL	0.30	0.35	0.34	--	0.32	0.33 ± 6%
(EOL-BOL)	-0.06	-0.01	-0.02	--	-0.04	-0.03 ± 59%
Cm-244 BOL	25.2	25.2	25.2	24.9	25.2	25.2
EOL	31.3	31.2	30.9	26.8	28.7	29.8 ± 6%
(EOL-BOL)	6.1	6.1	5.7	1.8	3.6	4.7 ± 37%
Cm-245 BOL	2.32	2.32	2.32	2.30	2.32	2.32
EOL	2.70	2.67	2.83	2.96	2.96	2.82 ± 4%
(EOL-BOL)	0.38	0.35	0.51	0.66	0.64	0.51 ± 25%
Cm-246 BOL	--	0.29	0.29	0.29	0.29	0.29
EOL	--	0.30	0.33	0.32	0.32	0.32 ± 3%
(EOL-BOL)	--	0.01	0.05	0.03	0.04	0.03 ± 46%

Table 27
Metal Core Comparison of reference toxicity characteristics
(all values in Cancer Dose)

ISOTOPE	EUROPE	JAPAN JENDL-2	JAPAN JENDL-3	RUSSIAN	UNITED STATES	MEAN VALUE
<i>BOL Uranium</i>						30.7
<i>EOL Uranium</i>	48.6	30.2	30.2	29.3	45.8	36.8 ± 23%
Np-237						
BOL						3.32E4
EOL	2.99E4	2.99E4	2.97E4	2.98E4	2.99E4	2.98E4±0.3%
Pu-238						
BOL						1.89E8
EOL	2.35E8	2.51E8	2.52E8	2.45E8	2.47E8	2.46E8±2%
Pu-239						
BOL						3.76E7
EOL	3.52E7	3.52E7	3.52E7	3.48E7	3.53E7	3.51E7 ± 0.5%
Pu-240						
BOL						5.42E7
EOL	5.37E7	5.39E7	5.37E7	5.32E7	5.35E7	5.36 ± 0.4%
Pu-242						
BOL						1.84E5
EOL	1.96E5	1.93E5	1.91E5	1.88E5	1.91E5	1.92E5 ± 1%
Am-241						
BOL						1.06E8
EOL	1.15E8	1.11E8	1.13E8	1.15E8	1.13E8	1.13E8 ± 1%
Am-242m						
BOL						1.40E6
EOL	4.51E6	7.23E6	6.41E6	5.44E6	6.22E6	5.96E6 ± 15%
Am-243						
BOL						6.16E6
EOL	5.72E6	5.72E6	5.78E6	5.89E6	5.83E6	5.79E6 ± 1%
Cm-242						
BOL						9.14E5
EOL	1.89E8	1.04E8	9.00E7	8.73E7	8.73E7	1.12E8 ± 35%
Cm-244						
BOL						3.33E8
EOL	4.13E8	4.12E8	4.08E8	3.54E8	3.79E8	3.93E8 ±6%
<i>BOL Transuranics</i>						7.32E8
<i>EOL Transuranics</i>	1.06E9	9.84E8	9.64E8	9.00E8	9.31E8	9.68E8 ±6%
<i>Pu-241 + Am-241</i>	5.79E8	5.78 E8	5.81E5	5.77E8	5.83E8	5.80E8 ± 0.4%
<i>Pu-239 + Pu-240</i>	8.89E7	8.91E7	8.89E7	8.80E7	8.88E7	8.87E7 ± 0.4%
<i>Pu-241 + Am-241 + Np-237</i>	1.16E5	1.16E5	1.16E5	1.16E5	1.17E5	1.16E5 ± 0.3%

RZ geometry

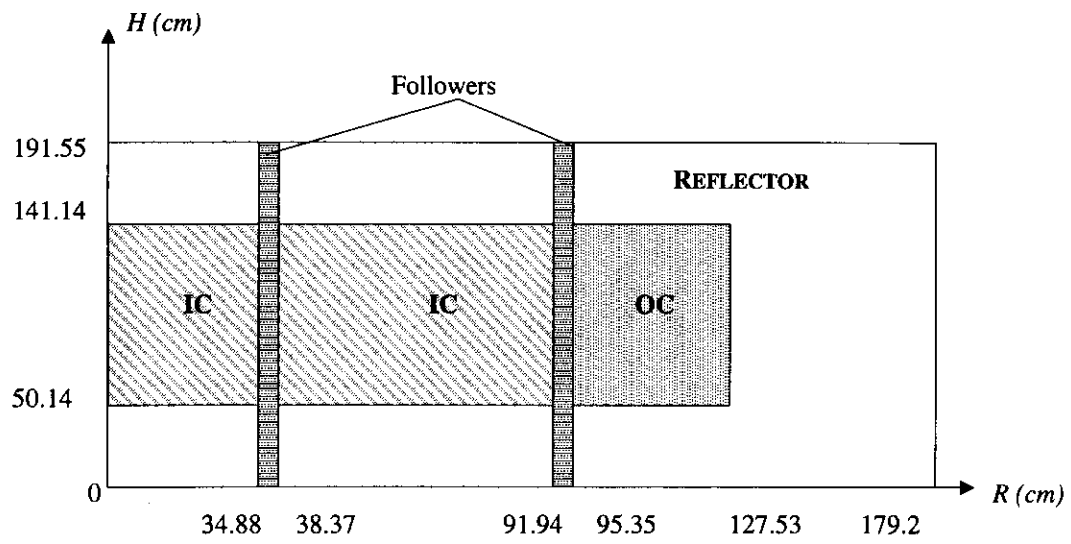
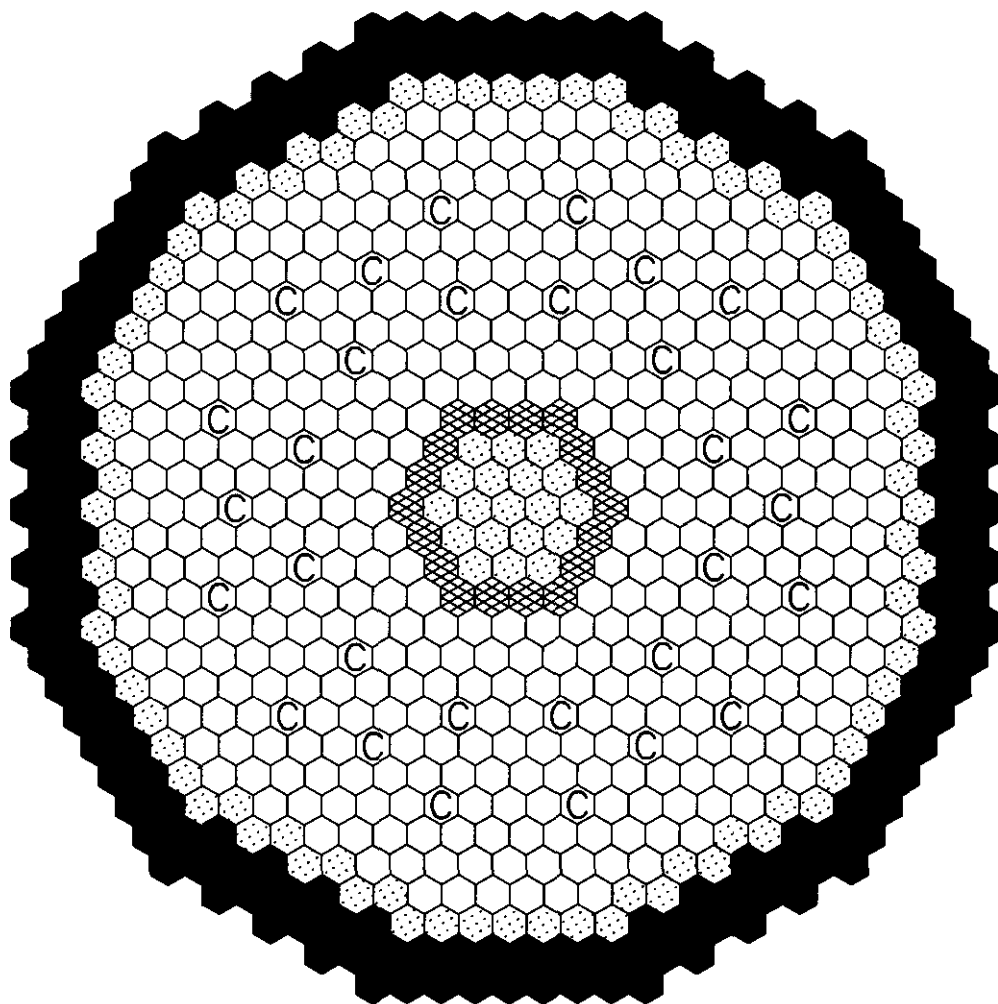


Figure 1 Oxide core geometry








- | | |
|--|---|
|  Driver Assembly (420) |  Control Assembly (30) |
|  Steel Reflector (103) |  Shield Assembly (186) |
|  B4C Exchange Assembly (18) | |

Figure 2 Metal benchmark reference core configuration

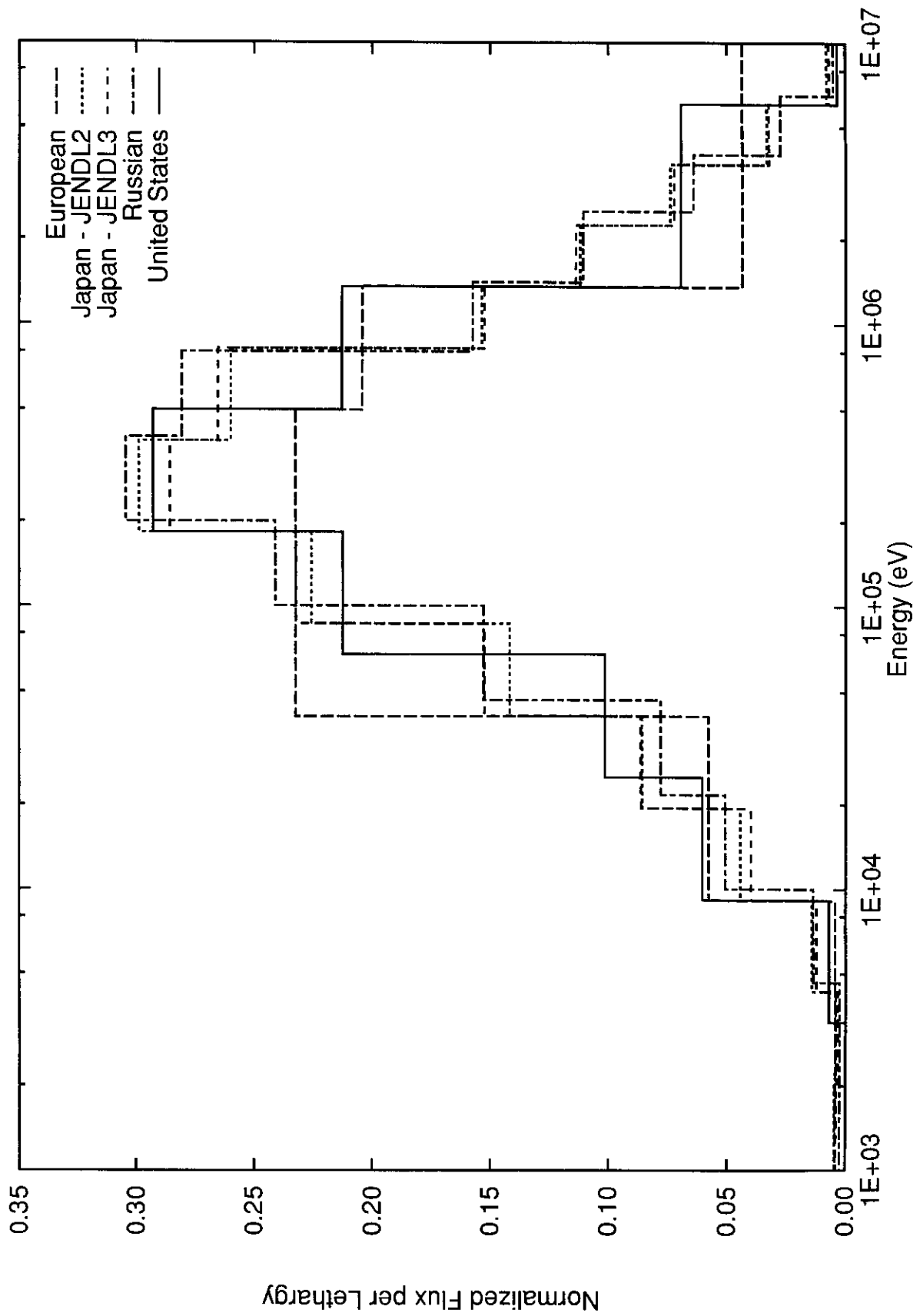


Figure 3 Comparison of spectra in the central core region

Appendix A

Specification of a fast plutonium-oxide burner reactor benchmark configuration (600 MWe)

Introduction

The present proposal is made in the frame of the NEA Nuclear Science Committee Working Party on the Physics of plutonium Recycling, as decided at the Paris meeting, 30-31 March 1993 [A.1].

The data necessary to the neutronics calculation are given both for the sub-assemblies and the core. Geometrical characteristics are given at 20°C, except for values of sections on **Cell calculations**, **Spatial calculations** and **Atomic number densities**, which correspond to operating conditions.

Fuel sub-assembly

- Fissile column height 900.0 mm
- Sub-assembly lattice dimension 151.4 mm
- Number of pins/sub-assembly 331 (221 fuel pins, 110 pins with no fuel)
- External clad diameter 6.55 mm
- Pellet diameter and central hole diameter 5.50 mm and 2.00 mm
- Nature and density of the fuel mixed UO_2 (10.46 g/cm³) - $\text{PuO}_{1.98}$ (10.94 g/cm³)
- Uranium isotopic composition

	U-235	U-238
at%	0.25	99.75

- Plutonium isotopic composition

	Pu-238	Pu-239	Pu-240	Pu-241	Pu-242	Am-241
at%	5.6	39.1	26.7	13.0	14.3	1.3

- Pu/U + Pu ratio for inner and outer cores 28.85% and 40.64% (mass)
- Composition and density of steel 7.95 g/cm³ (hexagonal tube and cladding)

	Fe	Cr	Ni	Mo	Mn
mass %	64.75	17.00	14.00	2.75	1.50

- Volume fraction of sub-assembly components

	UPuO₂	Steel	Sodium
volume %	22.96	23.11	33.89

- Number of subassemblies in inner and outer cores 128 / 112

Reflector sub-assembly

- Volume fraction of components

	Steel	Sodium
volume %	50.0	50.0

Control sub-assembly

- Absorber part not calculated
- Composition for the follower part

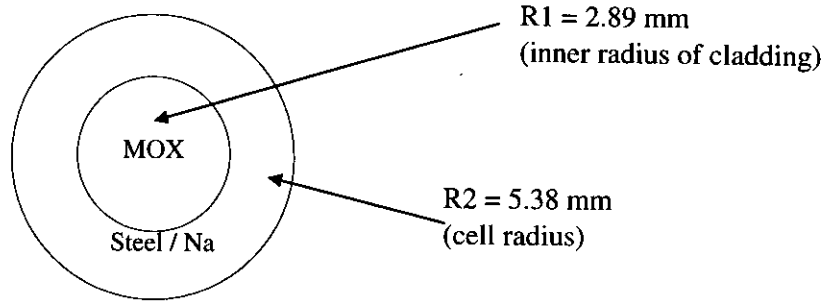
	Steel	Sodium
volume %	15.0	85.0

Operating conditions

- Thermal power 1500 MW
- Cycle length and load factor 125 EFPD and 0.80
- Residence time of fuel sub-assemblies 625 EFPD

Cell calculations

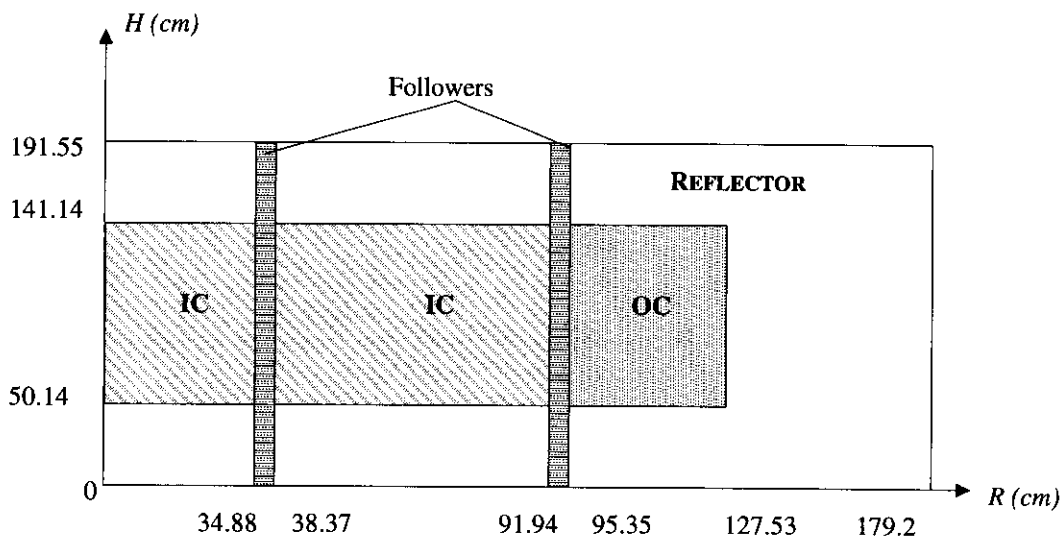
- Fuel cell – 1-D cylindrical cell with 2 zones
 - inner zone MOX fuel (temperature = 1227°C)
 - outer zone cladding, tube and sodium (temperature = 470°C)



- Rod follower, reflectors homogenised cells
- Atomic densities see Table A.1

Spatial calculations

- RZ geometry



- Mesh size ~ 5 cm, both R and Z
- Broad group structure ~ 30 groups
- Boundary conditions flux = 0 on the outer boundary

Atomic number densities

Table A.1

REGION	NUCLIDE	CELL CALCULATION INNER ZONE	CELL CALCULATION OUTER ZONE	HOMOGENISED ATOMIC DENSITY
<i>I N N E R C O R E I C</i>	U-235	3.268-E-05		9.409E-06
	U-238	1.304E-02		3.754E-03
	Pu-238	3.015E-04		8.683E-05
	Pu-239	2.097E-03		6.037E-04
	Pu-240	1.426E-03		4.105E-04
	Pu-241	6.913E-04		1.990E-04
	Pu-242	7.573E-04		2.180E-04
	Am-241	6.913E-05		1.990E-05
	Fe		1.728E-02	1.231E-02
	Cr		4.973E-03	3.541E-03
	Ni		3.627E-03	2.583E-03
	Mo		4.360E-04	3.105E-04
	O	3.672E-02		1.057E-02
	Na		1.038E-02*	7.389E-03
	Mn		4.153E-04	2.957E-04
<i>O U T E R C O R E O C</i>	U-235	2.743E-05		7.899E-06
	U-238	1.095E-02		3.152E-03
	Pu-238	4.247E-04		1.223E-04
	Pu-239	2.953E-03		8.503E-04
	Pu-240	2.008E-03		5.782E-04
	Pu-241	9.736E-05		2.803E-04
	Pu-242	1.067E-03		3.071E-04
	Am-241	9.736E-05		2.803E-05
	Fe		1.728E-02	1.231E-02
	Cr		4.973E-03	3.541E-03
	Ni		3.627E-03	2.583E-03
	Mo		4.360E-04	3.105E-04
	O	3.684E-02		1.061E-02
	Na		1.038E-02*	7.389E-03
	Mn		4.153E-04	2.957E-04
<i>A X I A L A N D R A D I A L S H I E L D I N G</i>	Fe			2.662E-02
	Cr			7.662E-03
	Ni			5.588E-03
	Mo			6.717E-04
	Na			1.093E-02
	Mn			6.398E-04
<i>R O D F O L L O W E R</i>	Fe			7.987E-03
	Cr			2.299E-03
	Ni			1.676E-03
	Mo			2.015E-04
	Na			1.863E-02
	Mn			1.920E-04

* 0. for the voided cell. See point 6 of section on **Required calculations (RZ geometry)**, page 49.

Required calculations (RZ geometry)

1. k-effective (in diffusion theory, possibly transport effects).
2. Critical balance components (PRODUCTIONS, ABSORPTIONS, LEAKAGE), and decomposition by isotope.
3. Spectrum indexes at core centre:

$$\frac{C(U-238)}{F(Pu-239)} ; \frac{F(U-238)}{F(Pu-239)} ; \frac{F(Pu-240)}{F(Pu-239)} ; \frac{F(Pu-241)}{F(Pu-239)}$$

4. Burnup calculation at a thermal power of $1500 \cdot 0.80$ MW, in three steps with flux calculation at each step:

0 EFPD	(beginning of life)
250 EFPD	(beginning of cycle)
375 EFPD	(end of cycle)
625 EFPD	(end of life)

Reactivity loss with breakdown into fission product and heavy isotope components.

5. Inner core and outer core isotopic compositions at the end of life (including minor actinide buildup).
6. Na void coefficient for inner core and whole core with breakdown into components (derived from perturbation theory calculations):
 - Axial leakage component,
 - Radial leakage component,
 - Scattering (spectral) component,
 - Absorption component,
 - Production component,

at beginning of life (BOL) and end of cycle (EOC).

7. Fuel Doppler reactivity at BOL and EOC, defined as:

$$k_{eff}^1 (T = 1227^\circ\text{C}) - k_{eff}^2 (T = 180^\circ\text{C}) / k_{eff}^1 \cdot k_{eff}^2$$

Decomposition by isotope.

8. Decay heat of irradiated fuel sub-assembly (IC and OC) at the end of the cycle and successive cooling times T_c :

$T_c = 1$ day, 1 month, 3 months, 1 year.

9. Neutron sources and activity of irradiated fuel assemblies.

10. Radiotoxicity of wastes at various cooling times (see annex to Appendix A):

$T_c = 0,$

$T_c = 100 \text{ y},$

$T_c = 1000 \text{ y},$

$T_c = 10000 \text{ y},$

$T_c = 100000 \text{ y},$

$T_c = 1000000 \text{ y},$

(hypothesis on reprocessing losses : 0.3% Pu and 1% minor actinides).

Reference

[A.1] OECD/NEA Report NEA/SEN/NSC/WPPR (93)3.

Radiotoxicity calculation

The calculation of the radiotoxicity will be performed as indicated below, starting from the isotopic composition of the discharged irradiated fuel ($T_c = 0$):

- Calculation of the mass of the descendants at various cooling time for each nuclide initially present in the wastes. The nuclides to be taken into account are plutonium (0.3% of the Pu content of the irradiated fuel), neptunium, americium and curium (1% of the minor actinide content of the irradiated fuel) and the fission products Tc-99, I-129 and Cs-135.
- Calculation of their respective activities in Bq.
- Calculation of the corresponding radiotoxicities and summation on the whole descendance for a given initial nuclide. The radiotoxicity is obtained when multiplying the activity by the hazard factor defined in Table A.2.

Table A.2 Hazard ingestion factors for oxide benchmark

NUCLIDE	HAZARD INGESTION FACTOR (Sv.Bq ⁻¹)
Ac-227+	3.9 E-6
Am-241	1.20 E-6
Am-242m+	1.14 E-6
Am-243+	1.19 E-6
Cm-242	3.54E-8
Cm-243	7.86 E-7
Cm-244	6.00 E-7
Cm-245	1.20 E-6
Cm-246	1.19 E-6
Cm-247+	1.11 E-6
Cm-248	4.40 E-6
Np-237+	1.06 E-6
Pa-231	2.89 E-6
Pb-210+	1.36 E-6
Pu-236	3.93 E-7
Pu-238	1.00 E-6
Pu-239+	1.16 E-6
Pu-240	1.16 E-6
Pu-241+	2.36 E-8
Pu-242	1.10 E-6
Pu-244+	1.08 E-6

NUCLIDE	HAZARD INGESTION FACTOR (Sv.Bq ⁻¹)
Ra-226+	3.05 E-7
Ra-228	3.40 E-7
Th-228+	2.00 E-7
Th-229+	1.05 E-6
Th-230	1.45 E-7
Th-232	7.40 E-7
U-232	3.44 E-7
U-233	7.20 E-8
U-234	7.20 E-8
U-235+	6.80 E-8
U-236	6.70 E-8
U-238+	6.70 E-8
Tc-99	3.4 E-10
I-129	7.4 E-8
Cs-135	1.9 E-9

+ indicates that the contribution of the short-life descendants is included.

Specification of metal-fuelled benchmark

This volume covers two aspects of this metal-fuelled burner benchmark:

- The beginning-of-life (BOL) core, and
- The once-through burner core.

I. Metal-fuelled burner start-up core benchmark

Introduction and goals

In this benchmark, the geometry and the beginning-of-life composition are specified.

Then, a beginning-of-life neutron balance is computed and compared among participants with the goal to assess the degree of spread in neutronics predictions and the reasons (e.g., differing cross-sections, leakage treatments, etc.) for the differences.

Then, a single depletion time step of specified duration and energy extraction is computed and both the end-of-cycle (EOC) composition and the end-of-cycle neutron balance are compared among participants with the goal to assess the degree of spread in burnup predictions. The depletion step is done with a fission product representation and (artificially) without fission product buildup so as to assess the contribution to differences in EOC neutron balance which can be attributed to different fission product treatments among the participants. *Note that for benchmark purposes the control rods are specified to (unphysically) remain fully withdrawn to the top of the fuelled region.*

This highly idealised benchmark is done preparatory to the subsequent benchmarks of **Metal-fuelled once-through burner core benchmark** (see following) and **Metal-fuelled multiple recycle burner core benchmark** (see Volume 5, Appendix B), which are more relevant to the plutonium burning issues. For this idealised case, the intercomparison differences reduce to cross-section and modelling effects alone when a specified geometry and BOL compositions are used. Alternately, in the subsequent benchmarks the beginning-of-equilibrium-cycle (BOEC) composition itself is adjusted by each participant to achieve an end-of-equilibrium-cycle (EOEC) eigenvalue of unity – and thus, the resulting BOEC composition will vary from participant to participant both because of differing eigenvalue, given a composition, and because of differing EOEC compositions, given a specified energy extraction per burn cycle.

Specification of model

Figure B.2 prescribes the geometry of the core.

Table B.1 prescribes the BOL composition by model region [B.1].

Table B.2 prescribes the burn cycle duration and energy extraction.

Basic data reporting

1. Identify the source of the basic nuclear data (e.g., ENDF/B-V) from which the cross-sections are generated;
2. Show broad group energy boundaries (express in energy at top of group);
3. Provide a narrative synopsis of the process for broad group cross-section preparation (e.g., state slowing down approximation, emission spectrum, choice of composition for collapse spectra, etc.).

BOL neutron balance reporting

1. Provide a narrative synopsis of the spatial representation (e.g., Hex-Z nodal, or if RZ, show dimensions; mesh sizes, etc.);
2. Identification of neutron balance solution algorithm (e.g., code name, type: finite difference, nodal, etc.);
3. BOL eigenvalue and convergence criterion;
4. Broad group flux spectrum at core centre (specify whether group flux or flux per unit lethargy);
5. k-infinity central (mesh or node) flux spectrum and core central (mesh or node) composition where:

$$k - \text{infinity} = \frac{\text{group sum of fission production}}{\text{group sum of absorption}}$$

6. Core leakage / core absorption -i.e., for “core” exclude blankets and reflectors);
7. Model leakage / model absorption (i.e., for “model” include all regions);
8. “Core” capture fractions; where denominator is group and isotope sum of absorption and numerators are:

All Heavy Metal, All Structural, Coolant

9. Energy-averaged cross-sections collapsed using central (mesh or node) fluxes $\langle\sigma_f\rangle$, $\langle v\sigma_f\rangle$, $\langle\sigma_f\rangle$ by TRU isotope.

Depletion methodology reporting

1. Description of the burnup chain representation
 - Diagram of isotopes considered,
 - Values of branching ratios, λ 's, etc.;
2. Provide a narrative description of how flux is normalised to prescribed power (e.g., fission only, fission + γ , etc.);
3. Provide a narrative synopsis of the burnup numerical solution process, e.g.,
 - Macro fitted vs. exposure – vis-à-vis number density solution of differential equations,
 - One vs. multi energy groups in the depletion equations,
 - Number of time steps and flux shape re-solution (if any),
 - Flux amplitude and time step renormalisations to constant power (if any),
 - Time advance numerical method (e.g., Runge Kutta), etc.);
4. Provide a narrative synopsis of the fission product representation.

BOL to EOC transition and EOC neutron balance reporting

1. Mass increments by isotope occurring as a result of the burnup step
 - Sum over entire model of change in mass, $\delta(\text{mass})$ by isotope,
 - Sum over entire model of $\delta(\text{mass})$ for the fission products;
2. EOC eigenvalue and convergence criterion;
3. Burnup swing = $(k_{\text{EOC}} - k_{\text{BOL}}) / (k_{\text{BOL}} k_{\text{EOC}})$;

4.

$$\text{TRU breeding ratio} = \frac{\text{EOC TRU mass summed over isotopes for whole model}}{\text{BOL TRU mass summed over isotopes for whole model}}$$

5. EOC neutron spectrum at core centre.

¹ Note that U-235 is excluded from this definition.

II. Metal-fuelled once-through burner core benchmark

Introduction and goals

In this benchmark, the geometry is specified. Also given are a $1/3$ core refuelling pattern, a specified time and energy extraction per burn cycle, and a specified composition (isotopic mass fractions) of a TRU feedstream coming from LWR spent fuel processing. Then, a fresh-fuel enrichment (TRU mass/ HM mass) is to be determined by each participant such that the EOEC reactor – comprised of one-cycle, two-cycle, and three-cycle burnt fuel assemblies – has an eigenvalue of 1.0 when all rods are withdrawn.

The edits of interest include:

- The fresh fuel enrichment (TRU mass)/ (Heavy Metal mass),
- The BOEC safety parameters (defined later),
- The rate of consumption of the TRU feedstock expressed in:
 - *Isotopic mass /MWe year,*
 - *Ci/MWe year,*
 - *Toxicity hazard /MWe year,*
 - *Watts/MWe year,*
- The rate of buildup of the LMR once-through spent fuel waste stream expressed in the same units.

The goal of this benchmark is to discover the spread in results among participants and, for the relevant “issues” – i.e., predictions of rate of reduction of LWR TRU and the buildup rate of LWR TRU and safety parameters – to sort out their sensitivity to the diversity of basic data and methods in use among the participants.

Specification of model

The geometry is unchanged from the previous benchmark and is given in Figure B.2. This again is the burner core with breeding ratio near to 0.5. For all non-fuel regions, the composition is given in Table B.1.

The isotopic fractions of the TRU from LWR spent fuel processing – which is to be used in fabricating fresh fuel assemblies is specified in Table B.3.

The burn cycle duration and energy extraction are unchanged from the previous benchmark and are given in Table B.2. *Note that for benchmark purposes the control rods are specified to (unphysically) remain fully withdrawn to the top of the fuelled region.*

The TRU/HM enrichment of fresh fuel assemblies is to be determined by each participant such that at EOEC the eigenvalue of the core comprised of one-cycle, two-cycle, and three-cycle burnt assemblies is 1.0 when all control rods are fully withdrawn to the top of the fuelled region.

BOEC neutron balance reporting

1. Narrative synopsis of the fuel management representation, e.g.,
 - Discrete representation of composition of fresh, once-burnt, and twice-burnt assemblies vs. spatially smeared representations,
 - fission product representation in partially burnt assemblies, etc.;
2. Fresh fuel enrichment = TRU/HM mass ratio.

BOEC to EOEC transition and mass flow reporting

1. Burnup swing = $(k_{EOEC} - k_{BOEC}) / k_{BOEC} k_{EOEC}$ } constant rod position

2.

$$\text{TRU breeding ratio} = \frac{\text{EOEC TRU mass inventory}}{\text{BOEC TRU mass inventory}}^2$$

3. Mass increments by heavy metal isotope:
 - Isotopic mass drawn from the LWR TRU for fabrication of the fresh fuel assemblies for each TRU isotope,
 - Sum over entire model of isotopic mass at BOEC for each TRU isotope,
 - Sum over entire model of change in mass, $\delta(\text{mass})$, due to burnup for each TRU isotope,
 - Sum over TRU isotopes of the previous item divided by the energy extraction (MWth days) delivered during the burn cycle;
4. Safety parameters reporting:
 - β_{eff} given in units of $\Delta k/k$,
 - Fuel Doppler coefficient i.e., of heavy metal isotopes (with a narrative synopsis of how the calculation is made and what isotopes are accounted for),
 - Sodium void worth
 - Of core (i.e., excluding blankets and reflectors),
 - Of core plus blanket /reflector regions above core,
 - Burnup swing of the cycle – defined above under BOEC to EOEC transition (with rods at constant position),
 - Decay heat level for decay times of 1 hour, 1 month, 1 year, 10 years, 10^2 years, 10^3 years, 10^4 years
 - Total,
 - Heavy metal component,
 - Fission product component;

² Note that this definition excludes U-235.

5. Radioactivity and decay:

- Provide a narrative synopsis of the radioactivity chain representation used for long-term out-of-core physics representations
 - *Isotopes treated,*
 - *Detailed chain representation specifically for the actinides showing all transitions and the values of all decay constants, branching ratios, etc.,*
- Describes the numerical solution approach for the equations,
- Describe how the decay heat is computed;

6. Curie increments at the times of 1, 10, 10^2 , 10^3 , 10^4 , 10^5 , 10^6 years from the time of BOEC:

- Isotopic mass $\cdot \lambda$ for the TRU masses drawn from the LWR TRU for fabrication of the fresh fuel assemblies for each TRU isotopes (expressed in Curies),
- Sum over entire model of BOEC mass $\cdot \lambda$ for each TRU isotope,
- Sum over entire model of $\delta(\text{mass}) \cdot \lambda$ by isotope for each TRU isotope,
- Sum over isotopes of the previous item divided by the energy extraction (MWth days) delivered during the burn cycle;

7. Toxicity hazard increments at the times of 1, 10, 10^2 , 10^3 , 10^4 , 10^5 , 10^6 years from the time of BOEC:

- $\{(\text{mass} \cdot (\lambda) \cdot (\text{Toxicity index})\}$ by isotope for each TRU isotope drawn from the LWR spent fuel for fabrication of the fresh fuel assemblies expressed in long-term cancer deaths via oral intake),
- Sum over the entire model of BOEC $\{(\text{mass} \cdot (\lambda) \cdot (\text{Toxicity index})\}$ by isotope for each TRU isotope expressed in long-term cancer deaths via oral intake,
- Sum over entire model of $\{(\text{mass} \cdot (\lambda) \cdot (\text{Toxicity index})\}$ by isotope for each TRU isotope,
- Sum over isotopes of the previous item divided by the energy extraction (MWth days) delivered during the burn cycle.

Reference

- [B.1] R. N. Hill, "Calculational Benchmark Comparisons for a Low Sodium Void Worth Actinide Burner Core Design", Proceedings of ANS Topical meeting on Advances in Reactor Physics, Charleston, SC., U.S.A., March 1992.

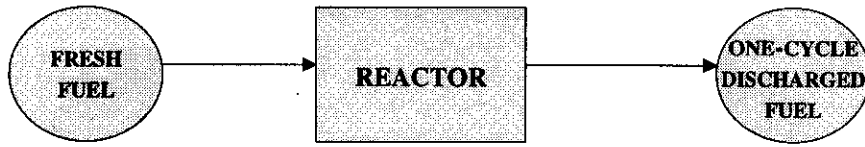


Figure B.1.1 LMR burner core benchmark

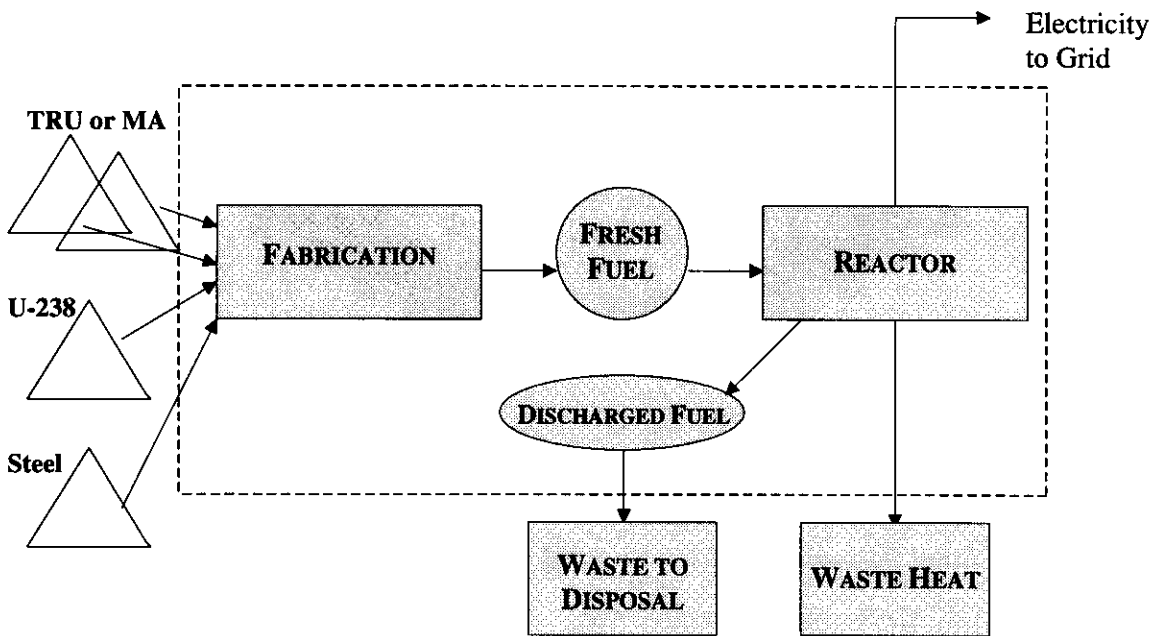
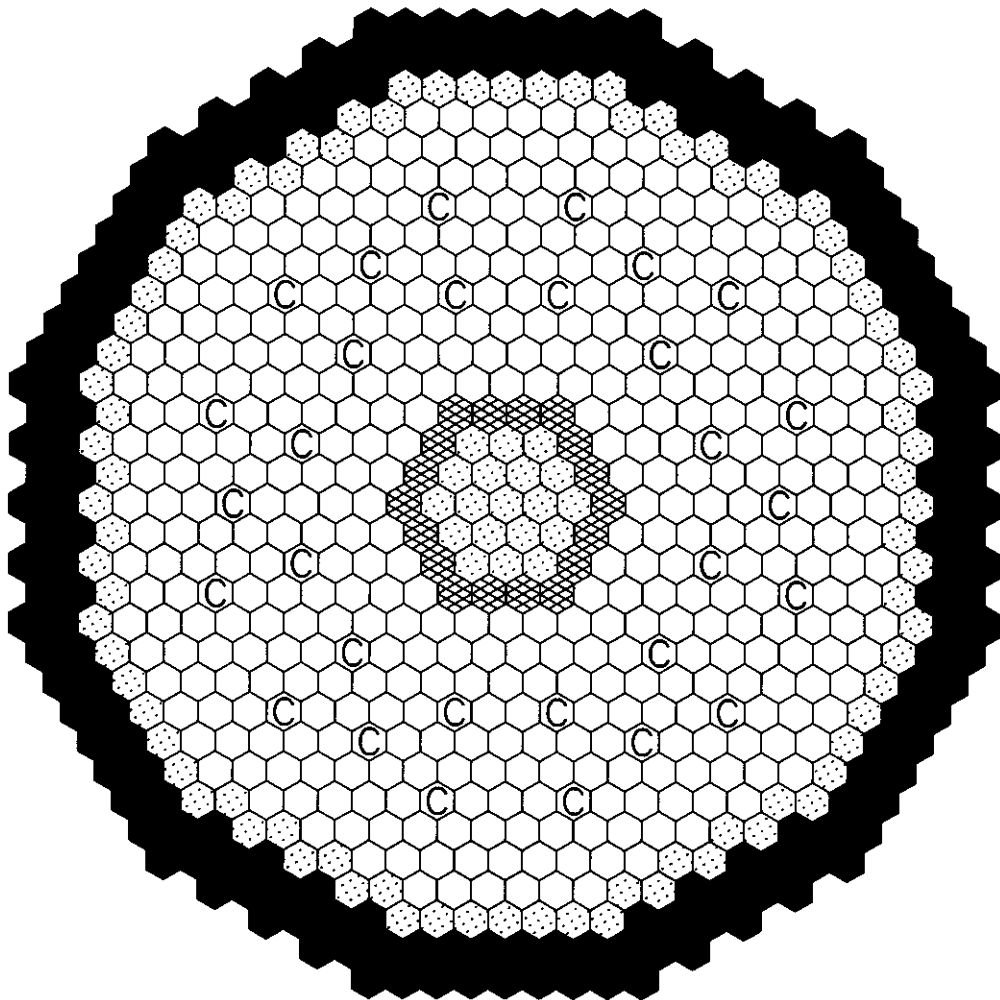


Figure B.1.II LMR once-through burner core benchmark



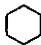




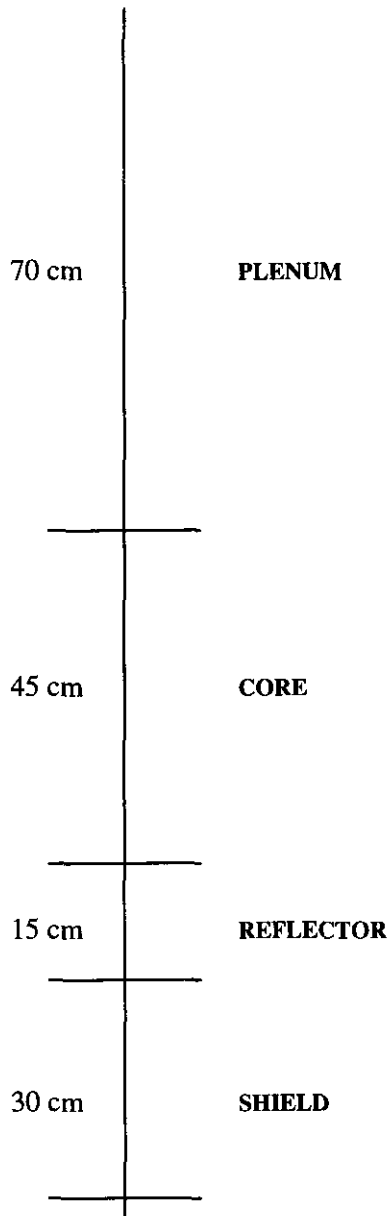
- | | |
|--|---|
|  Driver Assembly (420) |  Control Assembly (30) |
|  Steel Reflector (103) |  Shield Assembly (186) |
|  B4C Exchange Assembly (18) | |

Figure B.2 Geometry of breeding ratio ≈ 0.5 core [B.1]



All assemblies have an axial height of 160 cm with a 15.617 lattice pitch and are arranged in a configuration with 1/6 core symmetry, as shown on previous page. Only nine distinct material zones are specified. In the driver assemblies, a 30-cm thick lower axial shield is below a 15-cm thick lower reflector zone which is adjacent to the 45-cm tall active core; there is a 70-cm plenum region above the active core. The absorber regions of the control assemblies are parked above the active core. All other assemblies have uniform axial compositions. The isotopic number densities of each non-driver, non-blanket assembly region are specified in Table B.1 (see next). Table B.1 contains the driver and blanket compositions for the first benchmark only.

Figure B.2 (cont.) Geometry of breeding ratio ≈ 0.5 core [B.1]

Table B.1
Material composition specifications
(Number Densities in atoms/barn-cm)

ISOTOPE	DRIVER				CONTROL		EXCHANGE	REFLECTOR	SHIELD
	SHIELD	REFLECTOR	CORE	PLENUM	IN	OUT			
Na-23	7.447-3	7.447-3	7.637-3	1.678-2	8.865-3	2.080-2	6.075-3	3.546-3	3.546-3
Fe	1.179-2	4.821-2	1.790-2	1.790-2	1.538-2	4.865-3	1.405-2	6.088-2	1.516-2
Cr	1.761-3	7.201-3	2.674-3	2.674-3	2.297-3	7.265-4	2.100-3	9.092-3	2.263-3
Mo	7.952-5	3.252-4	1.207-4	1.207-4	1.038-4	3.281-5	9.485-5	4.106-4	1.022-4
Ni	6.499-5	2.658-4	9.868-5	9.868-5	8.479-5	2.681-5	7.751-5	3.356-4	8.354-5
Mn-55	2.777-5	1.136-4	4.217-5	4.217-5	3.624-5	1.146-5	3.313-5	1.434-4	3.570-5
B-10	9.278-3				2.783-2		8.017-3		9.495-3
B-11	3.758-2				3.092-3		3.247-2		3.845-2
C-12	1.171-2				7.731-3		1.012-2		1.199-2
Zr			3.189-3						
U-235			1.632-5						
U-238			8.144-3						
Np-237			1.521-4						
Pu-236			3.155-10						
Pu-238			2.845-5						
Pu-239			1.431-3						
Pu-240			5.606-4						
Pu-241			3.775-4						
Pu-242			1.093-4						
Am-241			7.071-5						
Am-242m			3.127-7						
Am-243			6.987-5						
Cm-242			2.741-8						
Cm-243			2.214-7						
Cm-244			1.555-5						
Cm-245			1.431-6						
Cm-246			1.778-7						

Table B.2
Fuel cycle assumptions

REACTOR SEGMENT OF CYCLE		
Cycle Length	365 days	
Capacity Factor	85%	
Power Rating	1575 MWth	
Core Driver Refuelling	$\frac{1}{3}$ per cycle	
Blanket Refuelling	$\frac{1}{4}$ per cycle	
RECYCLE SEGMENT OF CYCLE		
Cooling Interval	365 days	
Chemical Separation	done on day 1 of second year	
Blending & Fabrication	done on day 184 of second year	
Re-insertion into reactor	done on day 1 of third year	
CHEMICAL PARTITIONING FACTORS	<u>% to Product</u>	<u>% to Waste</u>
All TRU isotopes	99.9%	0.1%
Rare Earth Fission Products* (excluding Y, Sm, and Eu)	5%	95%
All Other Fission Products*	0%	100%

* Recommend for Benchmark purposes, recycle zero fission products and send all to waste.
ANL solutions are provided for recommended and for fission product recycle cases in the benchmark volume.

Table B.3
LWR transuranic isotopics

Isotopic values are the weight fraction of the individual isotope in the total transuranic mass

LWR	
ISOTOPE	AT 3.17 YEARS COOLING
Np-237	5.40-2
Pu-236	1.12-7
Pu-238	1.01-2
Pu-239	0.508
Pu-240	0.199
Pu-241	0.134
Pu-242	3.88-2
Am-241	2.51-2
Am-242m	1.11-4
Am-243	2.48-2
Cm-242	9.73-6
Cm-243	7.86-5
Cm-244	5.52-3
Cm-245	5.08-4
Cm-246	6.31-5
MA/fiss. Pu	0.172
MA/Pu	0.124
Np-237/MA	0.490
Am-241/MA	0.228
Am-243/MA	0.225
Np-chain	0.213

MA = sum of minor actinides;
fiss. Pu = Pu-239 + Pu-241;
Np-chain = Np-237 + Am-241 + Pu-241.

List of symbols and abbreviations

barns	nuclear physics' unit for measurement of cross-section $= 10^{-28} \text{ m}^2$
β_{eff}	effective delayed neutron fraction
Bq	becquerel, unit of activity of ionizing radiation source
BOEC BOL	<i>Beginning Of Equilibrium Cycle</i> <i>Beginning Of Life</i>
Ci	curie, radiation activity unit $1 \text{ Ci} = 3.7 \times 10^{10} \text{ Bq}$ (becquerel)
EFPD	equivalent full power days
EOC (EOEC) EOL	<i>End Of Cycle (End Of Equilibrium Cycle)</i> <i>End Of Life</i>
Δ, δ	variation
HM	heavy metal
k	neutron multiplication factor
λ	radioactive decay constant
LWR	<i>Light-Water Reactor</i>
MOX	<i>Mixed OXide</i> (uranium and plutonium)
MWe	megawatt electric
MWthd/kg	megawatt thermal days per kg of heavy metal
MWth	megawatt thermal
OECD/NEA	OECD Nuclear Energy Agency
Pu	plutonium
PUREX	<i>Plutonium Uranium EXtraction</i>
PYRØ	pyrometallurgical-based reprocessing
σ	standard deviation
S_n	discrete ordinates radiation transport method
Sv	sievert, unit for radioactive dose equivalent
TRU	Transuranium elements
TRUEX	<i>TRU EXtraction</i> American method for reprocessing spent fuel
U	uranium
WPPR	Working Party on Physics of Plutonium Recycling

**MAIN SALES OUTLETS OF OECD PUBLICATIONS
PRINCIPAUX POINTS DE VENTE DES PUBLICATIONS DE L'OCDE**

ARGENTINA – ARGENTINE

Carlos Hirsch S.R.L.
Galería Güemes, Florida 165, 4º Piso
1333 Buenos Aires Tel. (01) 331.1787 y 331.2391
Tel. (1) 331.1787
Telefax: (1) 331.1787

AUSTRALIA – AUSTRALIE

D.A. Information Services
648 Whitehorse Road, P.O.B 163
Mitcham, Victoria 3132 Tel. (03) 9873.4411
Telefax: (03) 9873.5679

AUSTRIA – AUTRICHE

Gerold & Co.
Graben 31
Wien 1 Tel. (0222) 533.50.14
Telefax: (0222) 512.47.31.29

BELGIUM – BELGIQUE

Jean De Lannoy
Avenue du Roi 202 Koningslaan
B-1060 Bruxelles Tel. (02) 538.51.69/538.08.41
Telefax: (02) 538.08.41

CANADA

Renouf Publishing Company Ltd.
1294 Algoma Road
Ottawa, ON K1B 3W8 Tel. (613) 741.4333
Telefax: (613) 741.5439

Stores:
61 Sparks Street
Ottawa, ON K1P 5R1 Tel. (613) 238.8985
211 Yonge Street
Toronto, ON M5B 1M4 Tel. (416) 363.3171
Telefax: (416)363.59.63

Les Éditions La Liberté Inc.
3020 Chemin Sainte-Foy
Sainte-Foy, PQ G1X 3V6 Tel. (418) 658.3763
Telefax: (418) 658.3763

Federal Publications Inc.
165 University Avenue, Suite 701
Toronto, ON M5H 3B8 Tel. (416) 860.1611
Telefax: (416) 860.1608

Les Publications Fédérales
1185 Université
Montréal, QC H3B 3A7 Tel. (514) 954.1633
Telefax: (514) 954.1635

CHINA – CHINE

China National Publications Import
Export Corporation (CNPIEC)
16 Gongti E. Road, Chaoyang District
P.O. Box 88 or 50
Beijing 100704 PR Tel. (01) 506.6688
Telefax: (01) 506.3101

CHINESE TAIPEI – TAIPEI CHINOIS

Good Faith Worldwide Int'l. Co. Ltd.
9th Floor, No. 118, Sec. 2
Chung Hsiao E. Road
Taipei Tel. (02) 391.7396/391.7397
Telefax: (02) 394.9176

**CZECH REPUBLIC – RÉPUBLIQUE
TCHEQUE**

Artia Pegas Press Ltd.
Narodni Trida 25
POB 825
111 21 Praha 1 Tel. (2) 2 46 04
Telefax: (2) 2 78 72

DENMARK – DANEMARK

Munksgaard Book and Subscription Service
35, Nørre Søgade, P.O. Box 2148
DK-1016 København K Tel. (33) 12.85.70
Telefax: (33) 12.93.87

EGYPT – ÉGYPTÉ

Middle East Observer
41 Sherif Street
Cairo Tel. 392.6919
Telefax: 360-6804

FINLAND – FINLANDE

Akateeminen Kirjakauppa
Keskuskatu 1, P.O. Box 128
00100 Helsinki
Subscription Services/Agence d'abonnements :
P.O. Box 23
00371 Helsinki Tel. (358 0) 121 4416
Telefax: (358 0) 121.4450

FRANCE

OECD/OCDE
Mail Orders/Commandes par correspondance:
2, rue André-Pascal
75775 Paris Cedex 16 Tel. (33-1) 45.24.82.00
Telefax: (33-1) 49.10.42.76
Telex: 640048 OCDE
Internet: Compté.PUBSINQ @ oecd.org

Orders via Minitel, France only/
Commandes par Minitel, France exclusivement :
36 15 OCDE

OECD Bookshop/Librairie de l'OCDE :
33, rue Octave-Feuillet
75016 Paris Tel. (33-1) 45.24.81.81
(33-1) 45.24.81.67

Dawson
B.P. 40
91121 Palaiseau Cedex Tel. 69.10.47.00
Telefax : 64.54.83.26

Documentation Française
29, quai Voltaire
75007 Paris Tel. 40.15.70.00

Economica
49 rue Héricart
75015 Paris Tel. 45.78.12.92
Telefax : 40.58.15.70

Gibert Jeune (Droit-Économie)
6, place Saint-Michel
75006 Paris Tel. 43.25.91.19

Librairie du Commerce International
10, avenue d'Iéna
75016 Paris Tel. 40.73.34.60

Librairie Dunod
Université Paris-Dauphine
Place du Maréchal de Lattre de Tassigny
75016 Paris Tel. 44.05.40.13

Librairie Lavoisier
11, rue Lavoisier
75008 Paris Tel. 42.65.39.95

Librairie des Sciences Politiques
30, rue Saint-Guillaume
75007 Paris Tel. 45.48.36.02

P.U.F.
49, boulevard Saint-Michel
75005 Paris Tel. 43.25.83.40

Librairie de l'Université
12a, rue Nazareth
13100 Aix-en-Provence Tel. (16) 42.26.18.08

Documentation Française
165, rue Garibaldi
69003 Lyon Tel. (16) 78.63.32.23

Librairie Decitre
29, place Bellecour
69002 Lyon Tel. (16) 72.40.54.54

Librairie Sauramps
Le Triangle
34967 Montpellier Cedex 2 Tel. (16) 67.58.85.15
Telefax: (16) 67.58.27.36

A la Sorbonne Actual
23 rue de l'Hôtel des Postes
06000 Nice Tel. (16) 93.13.77.75
Telefax: (16) 93.80.75.69

GERMANY – ALLEMAGNE

OECD Publications and Information Centre
August-Bebel-Allee 6
D-53175 Bonn Tel. (0228) 959.120
Telefax: (0228) 959.12.17

GREECE – GRÈCE

Librairie Kauffmann
Mavrokordatou 9
106 78 Athens Tel. (01) 32.55.321
Telefax: (01) 32.30.320

HONG-KONG

Swindon Book Co. Ltd.
Astoria Bldg. 3F
34 Ashley Road, Tsimshatsui
Kowloon, Hong Kong Tel. 2376.2062
Telefax: 2376.0685

HUNGARY – HONGRIE

Euro Info Service
Margitsziget, Európa Ház
1138 Budapest Tel. (1) 111.62.16
Telefax: (1) 111.60.61

ICELAND – ISLANDE

Mál Mog Menning
Laugavegi 18, Pósthólf 392
121 Reykjavik Tel. (1) 552.4240
Telefax: (1) 562.3523

INDIA – INDE

Oxford Book and Stationery Co.
Scindia House
New Delhi 110001 Tel. (11) 331.5896/5308
Telefax: (11) 332.5993
17 Park Street
Calcutta 700016 Tel. 240832

INDONESIA – INDONÉSIE

Pdji-Lipi
P.O. Box 4298
Jakarta 12042 Tel. (21) 573.34.67
Telefax: (21) 573.34.67

IRELAND – IRLANDE

Government Supplies Agency
Publications Section
4/5 Harcourt Road
Dublin 2 Tel. 661.31.11
Telefax: 475.27.60

ISRAEL

Praedicta
5 Shatner Street
P.O. Box 34030
Jerusalem 91430 Tel. (2) 52.84.90/1/2
Telefax: (2) 52.84.93

R.O.Y. International
P.O. Box 13056
Tel Aviv 61130 Tel. (3) 546 1423
Telefax: (3) 546 1442

Palestinian Authority/Middle East:
INDEX Information Services
P.O.B. 19502
Jerusalem Tel. (2) 27.12.19
Telefax: (2) 27.16.34

ITALY – ITALIE

Libreria Commissionaria Sansoni
Via Duca di Calabria 1/1
50125 Firenze Tel. (055) 64.54.15
Telefax: (055) 64.12.57

Via Bartolini 29
20155 Milano Tel. (02) 36.50.83
Editrice e Libreria Herder
Piazza Montecitorio 120
00186 Roma Tel. 679.46.28
Telefax: 678.47.51

Libreria Hoepli
Via Hoepli 5
20121 Milano
Tel. (02) 86.54.46
Telefax: (02) 805.28.86

Libreria Scientifica
Dott. Lucio de Biasio 'Aeiou'
Via Coronelli, 6
20146 Milano
Tel. (02) 48.95.45.52
Telefax: (02) 48.95.45.48

JAPAN – JAPON
OECD Publications and Information Centre
Landic Akasaka Building
2-3-4 Akasaka, Minato-ku
Tokyo 107
Tel. (81.3) 3586.2016
Telefax: (81.3) 3584.7929

KOREA – CORÉE
Kyobo Book Centre Co. Ltd.
P.O. Box 1658, Kwang Hwa Moon
Seoul
Tel. 730.78.91
Telefax: 735.00.30

MALAYSIA – MALAISIE
University of Malaya Bookshop
University of Malaya
P.O. Box 1127, Jalan Pantai Baru
59700 Kuala Lumpur
Malaysia
Tel. 756.5000/756.5425
Telefax: 756.3246

MEXICO – MEXIQUE
OECD Publications and Information Centre
Edificio INFOTEC
Av. San Fernando no. 37
Col. Toriello Guerra
Tlalpan C.P. 14050
Mexico D.F.
Tel. (525) 606 00 11 Extension 100
Fax : (525) 606 13 07

Revistas y Periódicos Internacionales S.A. de C.V.
Florencia 57 - 1004
Mexico, D.F. 06600
Tel. 207.81.00
Telefax: 208.39.79

NETHERLANDS – PAYS-BAS
SDU Uitgeverij Plantijnstraat
Externe Fondsen
Postbus 20014
2500 EA's-Gravenhage
Voor bestellingen:
Tel. (070) 37.89.880
Telefax: (070) 34.75.778

**NEW ZEALAND
NOUVELLE-ZELANDE**
GPLegislation Services
P.O. Box 12418
Thorndon, Wellington
Tel. (04) 496.5655
Telefax: (04) 496.5698

NORWAY – NORVÈGE
Narvesen Info Center – NIC
Bertrand Narvesens vei 2
P.O. Box 6125 Etterstad
0602 Oslo 6
Tel. (022) 57.33.00
Telefax: (022) 68.19.01

PAKISTAN
Mirza Book Agency
65 Shahrah Quaid-E-Azam
Lahore 54000
Tel. (42) 353.601
Telefax: (42) 231.730

PHILIPPINE – PHILIPPINES
International Booksource Center Inc.
Rm 179/920 Cityland 10 Condo Tower 2
HV dela Costa Ext cor Valero St.
Makati Metro Manila
Tel. (632) 817 9676
Telefax : (632) 817 1741

POLAND – POLOGNE
Ars Polona
00-950 Warszawa
Krakowskie Przedmieście 7
Tel. (22) 264760
Telefax : (22) 268673

PORTUGAL
Livraria Portugal
Rua do Carmo 70-74
Apart. 2681
1200 Lisboa
Tel. (01) 347.49.82/5
Telefax: (01) 347.02.64

SINGAPORE – SINGAPOUR
Gower Asia Pacific Pte Ltd.
Golden Wheel Building
41, Kallang Pudding Road, No. 04-03
Singapore 1334
Tel. 741.5166
Telefax: 742.9356

SPAIN – ESPAGNE
Mundi-Prensa Libros S.A.
Castelló 37, Apartado 1223
Madrid 28001
Tel. (91) 431.33.99
Telefax: (91) 575.39.98

Mundi-Prensa Barcelona
Consell de Cent No. 391
08009 – Barcelona
Tel. (93) 488.34.92
Telefax: (93) 487.76.59

Llibreria de la Generalitat
Palau Moja
Rambla dels Estudis, 118
08002 – Barcelona
(Subscripcions) Tel. (93) 318.80.12
(Publicacions) Tel. (93) 302.67.23
Telefax: (93) 412.18.54

SRI LANKA
Centre for Policy Research
c/o Colombo Agencies Ltd.
No. 300-304, Galle Road
Colombo 3
Tel. (1) 574240, 573551-2
Telefax: (1) 575394, 510711

SWEDEN – SUÈDE
CE Fritzes AB
S-106 47 Stockholm
Tel. (08) 690.90.90
Telefax: (08) 20.50.21

Subscription Agency/Agence d'abonnements :
Wennergren-Williams Info AB
P.O. Box 1305
171 25 Solna
Tel. (08) 705.97.50
Telefax: (08) 27.00.71

SWITZERLAND – SUISSE
Maditec S.A. (Books and Periodicals - Livres
et périodiques)
Chemin des Palettes 4
Case postale 266
1020 Renens VD 1
Tel. (021) 635.08.65
Telefax: (021) 635.07.80

Librairie Payot S.A.
4, place Pépinet
CP 3212
1002 Lausanne
Tel. (021) 320.25.11
Telefax: (021) 320.25.14

Librairie Unilivres
6, rue de Candolle
1205 Genève
Tel. (022) 320.26.23
Telefax: (022) 329.73.18

Subscription Agency/Agence d'abonnements :
Dynapresse Marketing S.A.
38 avenue Vibert
1227 Carouge
Tel. (022) 308.07.89
Telefax: (022) 308.07.99

See also – Voir aussi :
OECD Publications and Information Centre
August-Bebel-Allee 6
D-53175 Bonn (Germany)
Tel. (0228) 959.120
Telefax: (0228) 959.12.17

THAILAND – THAÏLANDE
Suksit Siam Co. Ltd.
113, 115 Fuang Nakhon Rd.
Opp. Wat Rajbopith
Bangkok 10200
Tel. (662) 225.9531/2
Telefax: (662) 222.5188

TURKEY – TURQUIE
Kültür Yayınları Is-Türk Ltd. Sti.
Atatürk Bulvarı No. 191/Kat 13
Kavaklıdere/Ankara
Dolmabahçe Cad. No. 29
Besiktas/Istanbul
Tel. 428.11.40 Ext. 2458
Tel. (312) 260 7188
Telex: (312) 418 29 46

UNITED KINGDOM – ROYAUME-UNI
HMSO
Gen. enquiries
Postal orders only:
P.O. Box 276, London SW8 5DT
Personal Callers HMSO Bookshop
49 High Holborn, London WC1V 6HB
Tel. (171) 873 8416
Telefax: (171) 873 8416
Branches at: Belfast, Birmingham, Bristol,
Edinburgh, Manchester

UNITED STATES – ÉTATS-UNIS
OECD Publications and Information Center
2001 L Street N.W., Suite 650
Washington, D.C. 20036-4910
Tel. (202) 785.6323
Telefax: (202) 785.0350

VENEZUELA
Libreria del Este
Avda F. Miranda 52, Aptdo. 60337
Edificio Galipán
Caracas 106
Tel. 951.1705/951.2307/951.1297
Telegram: Libreste Caracas

Subscriptions to OECD periodicals may also be placed through main subscription agencies.

Les abonnements aux publications périodiques de l'OCDE peuvent être souscrits auprès des principales agences d'abonnement.

Orders and inquiries from countries where Distributors have not yet been appointed should be sent to: OECD Publications Service, 2 rue André-Pascal, 75775 Paris Cedex 16, France.

Les commandes provenant de pays où l'OCDE n'a pas encore désigné de distributeur peuvent être adressées à : OCDE, Service des Publications, 2, rue André-Pascal, 75775 Paris Cedex 16, France.

10-1995